

PROCEEDINGS OF SPIE

High Contrast Metastructures II

Connie J. Chang-Hasnain
Fumio Koyama
Alan Eli Willner
Weimin Zhou
Editors

5–7 February 2013
San Francisco, California, United States

Sponsored and Published by
SPIE

Volume 8633

Proceedings of SPIE 0277-786X, V. 8633

SPIE is an international society advancing an interdisciplinary approach to the science and application of light.

High Contrast Metastructures II, edited by Connie J. Chang-Hasnain, Fumio Koyama,
Alan Eli Willner, Weimin Zhou, Proc. of SPIE Vol. 8633, 863313 · © 2013 SPIE
CCC code: 0277-786X/13/\$18 · doi: 10.1117/12.2021965

Proc. of SPIE Vol. 8633 863313-1

The papers included in this volume were part of the technical conference cited on the cover and title page. Papers were selected and subject to review by the editors and conference program committee. Some conference presentations may not be available for publication. The papers published in these proceedings reflect the work and thoughts of the authors and are published herein as submitted. The publisher is not responsible for the validity of the information or for any outcomes resulting from reliance thereon.

Please use the following format to cite material from this book:

Author(s), "Title of Paper," in *High Contrast Metastructures II*, edited by Connie J. Chang-Hasnain, Fumio Koyama, Alan Eli Willner, Weimin Zhou, Proceedings of SPIE Vol. 8633 (SPIE, Bellingham, WA, 2013) Article CID Number.

ISSN: 0277-786X

ISBN: 9780819494023

Published by

SPIE

P.O. Box 10, Bellingham, Washington 98227-0010 USA

Telephone +1 360 676 3290 (Pacific Time) · Fax +1 360 647 1445

SPIE.org

Copyright © 2013, Society of Photo-Optical Instrumentation Engineers.

Copying of material in this book for internal or personal use, or for the internal or personal use of specific clients, beyond the fair use provisions granted by the U.S. Copyright Law is authorized by SPIE subject to payment of copying fees. The Transactional Reporting Service base fee for this volume is \$18.00 per article (or portion thereof), which should be paid directly to the Copyright Clearance Center (CCC), 222 Rosewood Drive, Danvers, MA 01923. Payment may also be made electronically through CCC Online at copyright.com. Other copying for republication, resale, advertising or promotion, or any form of systematic or multiple reproduction of any material in this book is prohibited except with permission in writing from the publisher. The CCC fee code is 0277-786X/13/\$18.00.

Printed in the United States of America.

Publication of record for individual papers is online in the SPIE Digital Library.



SPIDigitalLibrary.org

Paper Numbering: Proceedings of SPIE follow an e-First publication model, with papers published first

online and then in print and on CD-ROM. Papers are published as they are submitted and meet publication criteria. A unique, consistent, permanent citation identifier (CID) number is assigned to each article at the time of the first publication. Utilization of CIDs allows articles to be fully citable as soon as they are published online, and connects the same identifier to all online, print, and electronic versions of the publication. SPIE uses a six-digit CID article numbering system in which:

- The first four digits correspond to the SPIE volume number.
- The last two digits indicate publication order within the volume using a Base 36 numbering system employing both numerals and letters. These two-number sets start with 00, 01, 02, 03, 04, 05, 06, 07, 08, 09, 0A, 0B ... 0Z, followed by 10-1Z, 20-2Z, etc.

The CID Number appears on each page of the manuscript. The complete citation is used on the first page, and an abbreviated version on subsequent pages. Numbers in the index correspond to the last two digits of the six-digit CID Number.

Contents

- vii *Conference Committee*
- ix *Introduction*
- xi Group IV photonics for the mid infrared (Plenary Paper) [8629-1]
R. Soref, The Univ. of Massachusetts at Boston (United States)
- xxvii Light in a twist: optical angular momentum (Plenary Paper) [8637-2]
M. J. Padgett, Univ. of Glasgow (United Kingdom)

HARNESSING LIGHT

- 8633 02 **Double photonic crystal vertical-cavity surface-emitting lasers (Invited Paper)** [8633-2]
P. Viktorovitch, Institut des Nanotechnologies de Lyon, CNRS, Univ. de Lyon (France);
C. Sciancalepore, Institut des Nanotechnologies de Lyon, CNRS, Univ. de Lyon (France)
and CEA-LETI Minatec (France); B. B. Bakir, CEA-LETI Minatec (France); X. Letartre,
C. Seassal, Institut des Nanotechnologies de Lyon, CNRS, Univ. de Lyon (France)
- 8633 03 **Physics of high contrast gratings: a band diagram insight** [8633-3]
W. Yang, C. J. Chang-Hasnain, Univ. of California, Berkeley (United States)

SLOW LIGHT

- 8633 05 **Demonstration of a slow-light high-contrast metastructure cage waveguide (Invited Paper)**
[8633-5]
W. Zhou, G. Dang, M. Taysing-Lara, U.S. Army Research Lab. (United States);
C. Chang-Hansnain, Univ. of California, Berkeley (United States)

VCSELS

- 8633 08 **Speed enhancement in VCSELS employing grating mirrors (Invited Paper)** [8633-8]
I.-S. Chung, J. Mørk, Technical Univ. of Denmark (Denmark)
- 8633 09 **VCSELS with a high-index-contrast grating for mode-division multiplexing** [8633-9]
Q. Ran, J. Mørk, Technical Univ. of Denmark (Denmark)
- 8633 0A **Rigorous, highly-efficient optical tools for HCG-VCSEL design (Invited Paper)** [8633-10]
P. Debernardi, R. Orta, Politecnico di Torino (Italy); W. Hofmann, Technische Univ. Berlin
(Germany)
- 8633 0B **Fano resonances GaN-based high contrast grating surface-emitting lasers** [8633-11]
T.-T. Wu, S.-H. Wu, T.-C. Lu, H.-C. Kuo, S.-C. Wang, National Chiao Tung Univ. (Taiwan)

NOVEL PHYSICS

- 8633 0D **Novel diffraction properties of high-contrast gratings (Invited Paper)** [8633-13]
B. Pesala, M. Madhusudan, CSIR - Central Electronics Engineering Research Institute (India)

BEAM STEERING

- 8633 0E **Super-high resolution beam steering based on Bragg reflector waveguides with high-contrast metastructures (Invited Paper)** [8633-14]
F. Koyama, X. Gu, Tokyo Institute of Technology (Japan)
- 8633 0F **Optical phased array using single crystalline silicon high-contrast-gratings for beamsteering (Invited Paper)** [8633-15]
B.-W. Yoo, Univ. of California, Berkeley (United States); T. Chan, Univ. of California, Davis (United States); M. Megens, T. Sun, W. Yang, Y. Rao, Univ. of California, Berkeley (United States); D. A. Horsley, Univ. of California, Davis (United States); C. J. Chang-Hasnain, M. C. Wu, Univ. of California, Berkeley (United States)
- 8633 0G **Optical phased array using high-contrast grating all-pass filters for fast beam steering** [8633-16]
W. Yang, T. Sun, Y. Rao, Univ. of California, Berkeley (United States); T. Chan, M. Megens, Univ. of California, Davis (United States); B.-W. Yoo, Univ. of California, Berkeley (United States); D. A. Horsley, Univ. of California, Davis (United States); M. C. Wu, C. J. Chang-Hasnain, Univ. of California, Berkeley (United States)

NOVEL FUNCTIONS

- 8633 0M **High contrast gratings for high-precision metrology (Invited Paper)** [8633-22]
S. Kroker, S. Steiner, T. Käsebier, E.-B. Kley, A. Tünnermann, Friedrich-Schiller-Univ. Jena (Germany)
- 8633 0N **High contrast grating mirrors for radiation-pressure optomechanics (Invited Paper)** [8633-23]
U. Kemiktarak, M. Durand, National Institute of Standards and Technology (United States) and Univ. of Maryland (United States); C. Stambaugh, J. Lawall, National Institute of Standards and Technology (United States)
- 8633 0O **Broadband quarter-wave plates at near-infrared using high-contrast gratings (Invited Paper)** [8633-24]
M. Mutlu, A. E. Akosman, G. Kurt, M. Gokkavas, E. Ozbay, Bilkent Univ. (Turkey)

INTEGRATED OPTICS

- 8633 0S **Silicon grating structures for optical fiber interfacing and III-V/silicon opto-electronic components (Invited Paper)** [8633-28]
G. Roelkens, Univ. Gent (Belgium); D. Vermeulen, Acacia Communications Inc. (United States); Y. Li, M. Muneeb, N. Hattasan, E. Ryckeboer, Y. Deconinck, D. Van Thourhout, R. Baets, Univ. Gent (Belgium)

- 8633 0U **Optical multiplexer using vertical coupler based on high contrast metastructure** [8633-30]
L. Zhu, W. Yang, C. J. Chang-Hasnain, Univ. of California, Berkeley (United States)

FILTERS AND DETECTORS

- 8633 0V **Cavity-resonator-integrated guided-mode resonance filters (Invited Paper)** [8633-31]
S. Ura, Kyoto Institute of Technology (Japan); K. Kintaka, National Institute of Advanced Industrial Science and Technology (Japan); J. Inoue, K. Nishio, Y. Awatsuji, Kyoto Institute of Technology (Japan)
- 8633 0W **Angular sensitivity of guided mode resonant filters in classical and conical mounts (Invited Paper)** [8633-32]
D. W. Peters, R. R. Boye, S. A. Kemme, Sandia National Labs. (United States)
- 8633 0Y **Tunable resonant-cavity-enhanced photodetector with double high-index-contrast grating mirrors** [8633-34]
S. Learkthanakhachon, K. Yvind, I.-S. Chung, Technical Univ. of Denmark (Denmark)
- 8633 0Z **Asymmetric direction selective filter elements based on high-contrast gratings** [8633-35]
S. Steiner, S. Kroker, T. Käsebier, D. Voigt, J. Fuchs, Friedrich-Schiller-Univ. Jena (Germany); F. Fuchs, Fraunhofer-Institut für Angewandte Optik und Feinmechanik (Germany); E.-B. Kley, Friedrich-Schiller-Univ. Jena (Germany); A. Tünnermann, Friedrich-Schiller-Univ. Jena (Germany) and Fraunhofer-Institut für Angewandte Optik und Feinmechanik (Germany)
- 8633 10 **Suspended Si/air high contrast subwavelength gratings for long-wavelength infrared reflectors** [8633-36]
J. M. Foley, J. D. Phillips, Univ. of Michigan (United States)

Author Index

Conference Committee

Symposium Chair

David L. Andrews, University of East Anglia Norwich (United Kingdom)

Symposium Cochairs

Alexei L. Glebov, OptiGrate Corporation (United States)

Klaus P. Streubel, OSRAM AG (Germany)

Program Track Chair

Ali Adibi, Georgia Institute of Technology (United States)

Conference Chairs

Connie J. Chang-Hasnain, University of California, Berkeley
(United States)

Fumio Koyama, Tokyo Institute of Technology (Japan)

Alan Eli Willner, The University of Southern California (United States)

Weimin Zhou, U.S. Army Research Laboratory (United States)

Conference Program Committee

Markus Christian Amann, Walter Schottky Institut (Germany)

Il-Sug Chung, Technical University of Denmark (Denmark)

David Fattal, Hewlett-Packard Laboratories (United States)

Weiwei Hu, Peking University (China)

Ernst-Bernhard Kley, Friedrich-Schiller-Universität Jena (Germany)

Philippe Lalanne, Institut d'Optique (France)

Rainer F. Mahrt, IBM Zürich Research Laboratory (Switzerland)

Pierre Viktorovitch, Ecole Centrale de Lyon (France)

Ming C. Wu, University of California, Berkeley (United States)

Session Chairs

1 Harnessing Light

Fumio Koyama, Tokyo Institute of Technology (Japan)

Ming C. Wu, University of California, Berkeley (United States)

2 Slow Light

Fumio Koyama, Tokyo Institute of Technology (Japan)

- 3 VCSELS
Roel G. Baets, University Gent (Belgium)
- 4 Novel Physics
David W. Peters, Sandia National Laboratories (United States)
- 5 Beam Steering
David Fattal, Hewlett-Packard Laboratories (United States)
- 6 Novel Lenses
Pierre Viktorovitch, Ecole Centrale de Lyon (France)
- 7 Novel Functions
Raffaele Colombelli, Institut d'Électronique Fondamentale (France)
- 8 Metastructures
Ekmel Ozbay, Bilkent University (Turkey)
- 9 Integrated Optics
Pierre Viktorovitch, Ecole Centrale de Lyon (France)
- 10 Filters and Detectors
Weidong Zhou, The University of Texas at Arlington (United States)

Introduction

Optical structures that are on the order of optical wavelength have been used to change the optical properties of the structures, similar to the use of nanostructures for quantization of electron wave. Recently, a new class of single planar layer subwavelength metastructures has emerged. The new metastructures are dielectric gratings with a large index contrast that can be designed to exhibit many extraordinary properties. For example, high contrast gratings (HCG) can provide very high reflection over a broad spectral range for light propagating in the direction orthogonal to the periodicity. It can also be designed to be a resonator with an extremely high quality factor and with user-friendly surface-normal coupling. Furthermore, changing the grating dimension individually, an ultra-thin lens or focusing reflector with high focusing power can be obtained.

This conference is the second one devoted to this theme. The presentations include a wide range of exciting advances, ranging from new physics, theories, to device applications. Various materials and fabrication technologies were used as basic platforms. In these proceedings, the readers will find discussion of novel direction selective filter elements, deep ultraviolet (DUV) polarizer and low noise infrared-mirrors. HCG designs to provide spatial mode filtering for mode control of VCSELs and wave-front-engineered mirrors are discussed. Phase engineering using HCG are explored in surface-normal transmission for solar cell concentrator optics and spiral lens applications. Using it at a glancing angle for hollow core waveguide, slow light waveguides are demonstrated. In addition, dynamically tunable all-pass filter array for fast optical beam steering is also presented.

During and post conference, we received much positive feedback and encouragement from attendees and presenters. There are genuine sense of excitements and enthusiasm about this topic, as evident by the full house attendance and many questions after each talk. We are grateful to all the attendees for asking many valuable questions. As always, the primary ingredient for a successful technical conference is the quality of the work presented by the contributors. We would like to thank all the contributors for the quality of their presentations, and their eagerness to share new information and discuss different point of views. We would like also to express our gratitude to all keynote and invited speakers for presenting exceptional overviews and igniting thought-provoking discussions. We are grateful to the committee members and session chairs, as their support and dedication before and during the event had a significant impact on the outcome and success of the meeting. We would like also to acknowledge the SPIE support staff, and our SPIE coordinator, for their invaluable help.

Connie J. Chang-Hasnain
Fumio Koyama
Alan Eli Willner
Weimin Zhou

Group IV photonics for the mid infrared

Richard Soref

Department of Physics and the Engineering Program

The University of Massachusetts at Boston, 100 Morrissey Boulevard, Boston, MA USA 02125

ABSTRACT

This paper outlines the challenges and benefits of applying silicon-based photonic techniques in the 2 to 5 μm mid-infrared (MIR) wavelength range for chem.-bio-physical sensing, medical diagnostics, industrial process control, environmental monitoring, secure communications, Ladar, active imaging, and high-speed communications at 2 μm . On-chip passive and active components, mostly waveguided, will enable opto-electronic CMOS or BiCMOS integrated “circuits” for system-on-a-chip applications such as spectroscopy and lab-on-a-chip. Volume manufacture in a silicon foundry is expected to yield low-cost (or even disposable) chips with benefits in size-weight-power and ruggedness. This is “long-wavelength optoelectronic integration on silicon” which we call LIOS. Room temperature operation appears feasible, albeit with performance compromises at 4 to 5 μm . In addition to the electronics layer (which may include RF wireless), a 3-D LIOS chip can include several inter-communicating layers utilizing the photonic, plasmonic, photonic-crystal and opto-electro-mechanical technologies. The LIOS challenge can be met by (1) discovering new physics, (2) employing “new” IV and III-V alloys, (3) scaling-up and modifying telecom components, and (4) applying nonlinear-optical wavelength conversion in some cases. This paper presents proposals for MIR chip spectrometers employing frequency-comb and Ge blackbody sources. Active heterostructures employing Si, Ge, SiGe, GeSn and SiGeSn are key for laser diodes, photodetectors, LEDs, switches, amplifiers, and modulators that provide totally monolithic foundry integration, while numerous III-V semiconductor MIR devices within the InGaAsSb and InGaAsP families offer practical hybrid integration on Si PICs. Interband cascade and quantum cascade lasers on Ge waveguides are important in this context.

Keywords: optoelectronics, photonic integration, silicon, germanium, SiGeSn, sensors, communications, plasmonics

1. INTRODUCTION

This paper outlines the opportunities for creating a fully integrated mid infrared (MIR) mini-system on a Si or SOI chip. The challenges are discussed and some attractive approaches are proposed. We shall define MIR (somewhat arbitrarily) as the wavelength region that extends from 2 to 5 μm , including thereby the 3- to-5 μm band wherein the atmosphere is transparent—a band that enables free-space as well as guided-wave applications.

The Si-based progress already attained in the telecommunications wavelength bands near 1.55 μm is an excellent launching point for the thrust into MIR. The last two decades have witnessed the emergence of Si-based passive and active waveguided components constructed from Si and Ge and from the alloys SiGe, GeSn and SiGeSn—components often in the form of electrically controlled group IV heterostructures. This technology-- spotlighted here-- is best described as “group IV photonics” rather than “silicon photonics.”

The expectation of high performance when migrating group IV photonics into the MIR is based upon the availability of: (1) elements-and-alloys that are transparent over large stretches of the near-to-far infrared spectrum, (2) electrically pumped MIR gain, (3) sensitive detection at MIR, (4) MIR electro refraction and electro absorption mechanisms, and (5) strong nonlinear MIR responses. Another key expectation is the volume manufacture of OEICs in a state-of-the-art silicon CMOS or BiCMOS foundry node. That hope is based on the recent commercially oriented success of foundry-fabricated “CMOS photonics” for active optical cables, optical interconnects, optical network structures, and hand-held optical/wireless devices. It can be inferred from the wide-spectrum group IV properties mentioned above that group IV photonics will have---in addition to MIR—a strong role to play in the longwave infrared and Terahertz zones, but those specifics are beyond the scope of this article.

Looking at the bigger picture of active photonics, it is important to note that InP-based integrated photonics is leading the “integration race” at telecom and is giving strong competition to group IV photonics in “non foundry” areas. That competition would still persist if and when the InP-based integration is extended to longer wavelengths. An important thesis of this paper is that discrete-device III-V heterostructures—appropriately designed for MIR—can be hybrid-integrated into or onto a group IV photonics layer, thus providing a very effective composite MIR layer. The hybrid active devices would use ternary and/or quaternary alloys within the InGaAsSb and InGaAsP families.

1.1 Outline of this paper

In some respects, the present paper is an update of my 2008 Photonics West paper¹ in which I suggested the acronym LIO. Today, I would update that acronym to LIOS signifying “long-wavelength integrated optoelectronics on silicon.” The present paper gives conceptual guidelines for LIOS, presents a mini-review of other people’s MIR work, and offers my proposals for chip spectrometers and other components. The next section illustrates how an MIR system of wired components would be condensed into a chip. Then the versatility and “ultimate” capability of 3D multi-technology MIR integration are described; then unusual materials are discussed. Potential applications of MIR OEIC chips are described and MIR waveguiding methods are outlined. Next we examine chip spectrometers and refractometers. Then we focus on hybrid integration and monolithic integration employing SiGeSn/SiGeSn heterostructures. Finally, we consider how nonlinear optical effects in group IV alloys and elements are applied to the MIR.

2. CHIP VERSUS WIRED-COMPONENTS SYSTEM

If we look at a typical prior-art MIR system, it is a collection of components interconnected electrically by wires and connected optically in free space by lenses and fibers. The drive transistors are included in the system as a chip or circuit board. All of this can, in principle, be condensed onto one planar Si chip to form an improved system as illustrated schematically in Figure 1 where we show two versions of the chip. The upper chip contains all of the optical processing within a network of waveguides, and the lower chip (which also has waveguides) couples optically to free space for

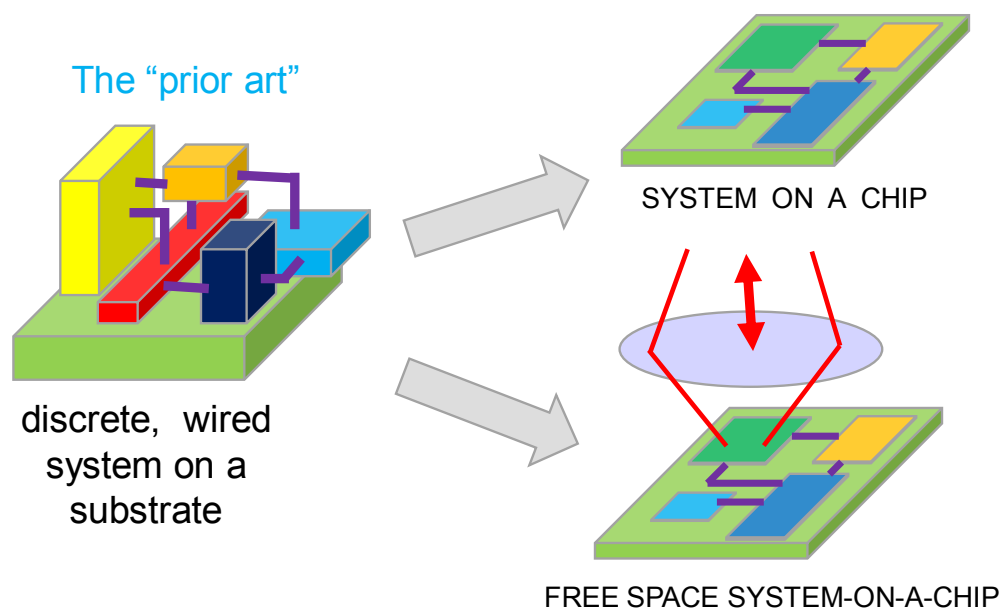


Figure 1. Transformation of a conventional prior-art MIR system into an MIR system-on-a-chip: either a totally waveguided chip, or a chip coupled optically to free space.

remote sensing, lidar, communications, etc. For free space uses, the on-chip MIR source could be a VCSEL and the receiver a surface-normal photodiode. Alternatively, both the MIR emitter and detector could be waveguided and would use a 2D surface grating (or a photonic-crystal Fano resonance structure) to couple inplane light out-to and in-from free space. Figure 1 indicates our motivations for the MIR chip: OE integration, cost savings through mass production, compactness, ruggedness, reliability, and savings in power and weight. The chip approach applies to newly designed

MIR systems but does not apply to all existing MIR wired systems. For example, some existing systems contain high output-power MIR lasers, and in those cases, the chip scenario is problematic because the chip would require extensive heat sinking. So the Figure-1 transformation covers some fraction of present systems. Returning for a moment to the free-space coupling, it is quite possible that the MIR chip could contain “meta material” plasmonic structures² that interact with normally incident free-space light; however we shall not cover that category of devices in this article because we want to emphasize instead on-chip waveguided networks. Figure 1 proposes a significant shrinkage of the wired system. It would be less demanding to convert the bulky system into a “multi chip module” on a silicon “bench” having centimeter-scale dimensions and several electronic chips (or MIR photonic chips) flip-chip bonded to the substrate. However, that kind of “intermediate” OE integration is not the “ultimate answer” being sought here.

2.1 Temperature of operation

Room-temperature operation is much preferred for the MIR chip. As the wavelength of operation is increased above 2 μm , the need for cooling the chip becomes more urgent. Room-temperature operation at 2 μm is definitely feasible but 300K operation at 5 μm is difficult in some systems. In MIR OEICs, temperature is not an issue for the on-chip *transistors* because they “do not care” what the wavelength of operation is. (That is why the trade name *CMOS photonics* applies also to MIR). Transistors will operate cooled if necessary. We endorse the idea of compromise to assure 300K viability at 4 to 5 μm . Some system performance should be sacrificed in order to operate uncooled. For example, a reduced detectivity of group IV or III-V PIN photodiodes could be accepted-- or uncooled microbolometers could be employed. For on-chip semiconductor laser diodes, a higher-than-normal injection-current density could be tolerated.

3. THE 3-D INTEGRATED MULTI-TECHNOLOGY CHIP

The original OEIC vision that I set forth in 1993 (Fig. 3 of my review article³) was an integration of CMOS (and/or Bipolar and HBT devices) with active and passive silicon photonic components in one or two SOI planes—which is in essence 2D integration. Since that time, many researchers have proposed more sophisticated versions of the OE chip that rely upon 3D layering or stacking in the chip: for example, MIT used two photonic layers in their near-infrared electronic-photonic chip. Another example comes from Michal Lipson’s group at Cornell. They have proposed silicon nitride waveguides in their telecom chip⁴, but the guides in their 3D OEIC could just as easily be Si or Ge when the chip is modified for MIR use. For electrical connections to the various active optical components, vertical through-silicon-vias (TSV) are employed in the 3D structure. I believe that an extremely capable and versatile 3D chip can be created by merging photonics technology in a synergistic way with plasmonic, photonic-crystal (PhC) and opto-electromechanical (OEM) technologies on the same chip. This proposal^{5,6} is shown in Figure 2. There can be independent layers of photonic, plasmonic, photonic-crystal, and OEM structures.

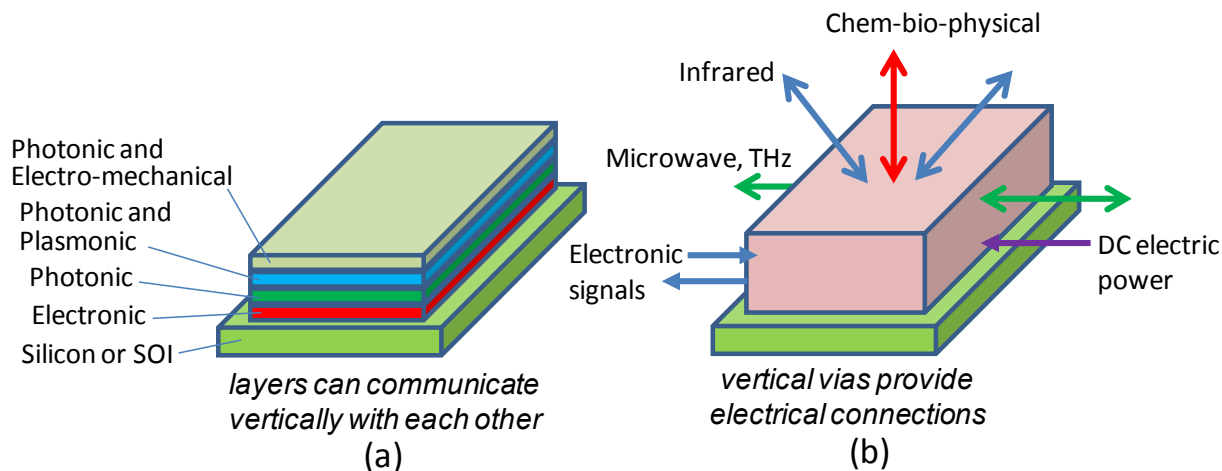


Figure 2. Proposal for the “ultimately capable” 3D-integrated MIR system on a chip showing the multiple possible technologies (left) and all the available inputs and outputs (right).

Or, technologies can be combined within one layer as indicated. Vertical interconnection or communications between layers is usually necessary. With its optical forbidden gap and slow light possibilities, the 2D photonic crystal layer offers special waveguiding in line-defect waveguides as well as in-layer waveguide couplings. There is of course the 3D PhC, but we shall leave that out of consideration here. As suggested in Figure 3b, the spatial inputs and outputs to the MIR chip encompass electrical, electronic, optical, microwave, and chem.-bio-physical “signals”. As final comment, let’s recognize that biological proteins can be deposited directly on an OEIC to create bio-photonic enabled electronics.

4. “UNUSUAL” GROUP IV MID INFRARED MATERIALS

Let’s look first at group IV materials that are not presently in the “mainstream” –materials that could contribute to group-IV MIR photonics over the longer term. The first two materials are porous silicon and porous germanium. Porous-Si MIR waveguides have already been implemented^{7,8}. There is also a group of monolayered materials consisting of Graphene^{9,10,11} and the unusual Silicene and Germanene materials,¹² both of which have MIR response. In addition, dense nano-crystalline silicon has been used for infrared waveguiding upon an SiO₂ layer. Diamond layers and structures have photonic applications over a wide spectrum including MIR, and nano-crystalline diamond is a practical implementation¹³. Amorphous Si may have MIR uses, and in Section 10 we point out that hydrogenated *a*-Si has significant NLO properties¹⁴. Noteworthy is an unusual binary alloy whose lattice parameter is close to that of Ge. The crystalline “dilute carbide” Ge_{1-x}C_x has MIR promise because (surprisingly) the bandgap is expected to decrease as a few percent of C is added to Ge. For an “isolated” carbon atom in a Ge host, the differing electronegativities of Ge and C produce an isoelectronic “deep level” E_d in the conduction band of GeC. As pointed out by Mark A. Wistey¹⁵, E_d “repels” the original conduction band E_c of GeC, creating new higher- and lower-energy conduction bands E⁺ and E⁻ via band anti-crossing. Thereby the dilute GeC becomes a *direct bandgap* material with E⁻ in the 0.5 – 0.6 eV range. Prof. Wistey is presently growing such GeC to demonstrate Si-based CMOS-compatible alloy for active band-to-band MIR devices.

Also in the “unusual” category is the short-period superlattice (SL) built up from atomic monolayers of Si and of Ge in an appropriate sequence. The strained layer SL of Si₂Ge₁₄ on bufferd Ge[100] is predicted¹⁶ to have an 0.77 eV *direct bandgap*, and I shall speculate that the doubly tensile strained SL of undoped Si₂Ge₁₄ when grown upon a GeSn buffer will have a direct MIR bandgap, ideal for LEDs. The hybrid of Graphene on Silicon works for opto electronics¹⁷, to which I would add Graphene on Ge. Silicene and Germanene are Graphene-like materials grown in nano-ribbons or epitaxial sheets⁹. Using either Si atoms or Ge atoms, the 2D hexagonal sheets of Silicene or Germanene have the planar honeycomb geometry of Graphene in their mono-atomic layers. It was shown recently that the mid-infrared absorbance of these three materials is essentially identical¹⁷, which implies on-chip photonic applications for these novel group IV materials.

5. POTENTIAL APPLICATIONS OF MIR SYSTEM-ON-A-CHIP

The principal applications are: chemical-biological-physical sensing, medical diagnostics, industrial process control, environmental monitoring, secure communications, Ladar, active imaging, free-space laser communications, infrared astronomy signal-combining¹⁸, invisible-fence alarm systems, sensor fusion, optical coherence tomography, and ultrafast fiber-optic communications at 2 μm (a rather new and significant direction.) Sensing is at the heart of the chem-bio-physico/medical/industrial/environmental thrusts and most of this paper addresses the ways in which sensor chips could be actualized. Sensors can be categorized according their read-in and readout arrangements (Section 5.2 below). The MIR applications of laser-comm, ladar and chem-bio sensing overlap with the ongoing CIPHER program sponsored by DARPA/MTO. Optical coherence tomography is a chip-based technique that can, I think, be “ported” easily from the near infrared to the MIR for medical application in intravascular imaging and ophthalmology¹⁹. Quantum information processing on Si²⁰ is possible in principle at MIR, but it is not clear that MIR offers advantages over 1.55 μm for photon correlations and single-photon generation.

5.1 Ultrafast optical communications at 2 μm for long-haul fiber-telco networks

“Exploding” internet traffic impacts fiber-optic networks around the world. Both the need for energy reduction and the demand for increased network capacity “cry out” for a solution in this decade. To address this issue, two R&D projects

have been funded in Europe: the Photonics Hyperhighway (EPSRC sponsor), and MODE-GAP (European Union sponsor). Relevant to this paper, one approach being taken is to deploy photonic-bandgap fibers in the 2 μm wavelength region (fibers currently offering 4.5 dB/km transmission loss) to achieve a significant increase in network capacity by supplementing the 1.31 and 1.55 μm infrastructure. For “node chips” within the ~2 μm network, the need arises to create ultrafast, low-energy 2 μm PICs containing semiconductor lasers and detectors and associated components. I believe that group IV OEICs would provide an excellent 2 μm chip solution -- a viable alternative to the European III-V semiconductor chip approach. By utilizing SOI-based Si, Ge, GeSn and SiGeSn integrated heterostructure photonics, a complete suite of room-temperature ultrafast 2 μm PIC/OEIC components (LD, PD, EOM, etc) could be developed for “all monolithic” foundry manufacture as illustrated in a patent²¹. Note that the laser diode source, a PIN MQW LD having undoped GeSn QWs and SiGeSn barriers, is likely to have higher wall-plug efficiency and lower threshold current than the heavily doped n⁺⁺ Ge-on-Si LD being developed for 1.55 μm. λ~2 μm is “natural” for GeSn technology.

5.2 Sensor Configurations

We have illustrated in Figure 3 a few specific sensor configurations out of the many possibilities. The free-space option (upper left) has transmitter and receiver co-located on chip. The disposable sensor (upper right) could have economic impact.

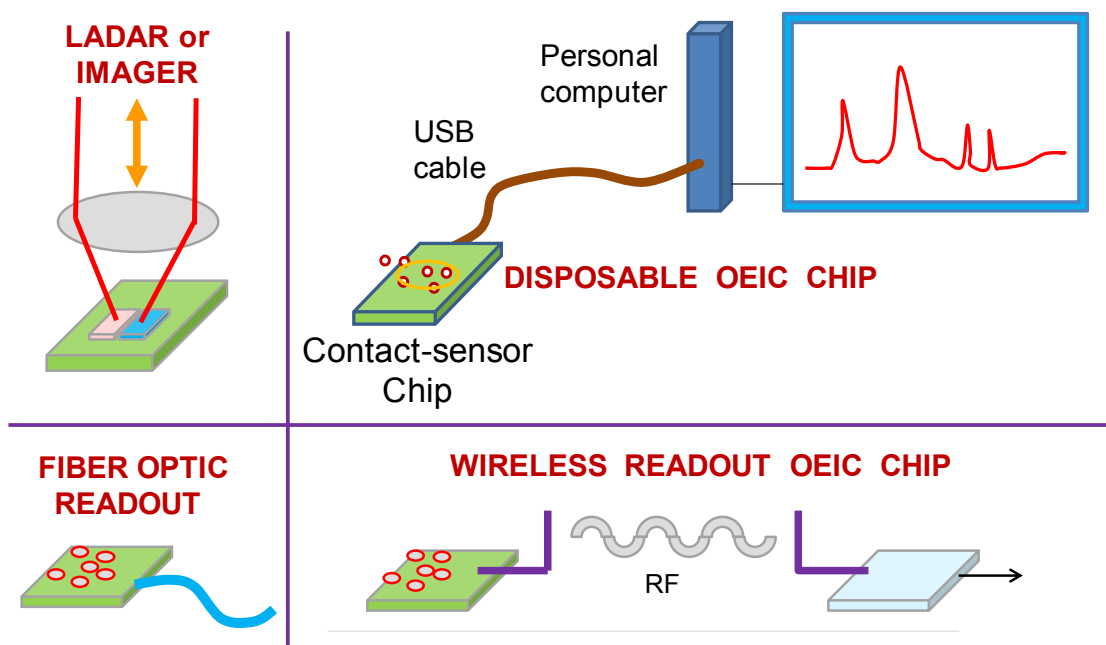


Figure 3. Several feasible configurations of MIR system chips showing optical couplings and readouts.

I’m suggesting that the low-cost OEIC “contact sensor” communicates with a hand-held or desk-top readout device via an “optical USB cable” that includes a dc electrical lead to power the PD and LD on chip. The lower left shows a remote sensor “head” in which bi-directional light accesses the sensor over fiber-optic coupling. The lower right shows how a sensor-OEIC communicates without wires to the readout station. An on-sensor wireless/RF transmitter or transceiver is quite feasible²² and will be very valuable in many situations for readout communications to-and-from the chip. Disposable chips are discussed on a web link²³.

6. MIR WAVEGUIDES, RESONATORS AND OTHER “PASSIVES”

As I outlined earlier^{1,24,25,26}, the principal MIR passive waveguided structures (strip channel waveguides, micro-ring-and-disk cavities, filters, directional couplers, WDM and WDDM structures) are silicon-on-insulator, silicon-on-sapphire, and silicon-on-nitride: SOI, SOS and SON. Today, all three approaches are supported by experimental results^{27,28,29}. (Regarding SOI, it interesting that the L1 PhC technique is valuable out to 3.9 μm³⁰). This waveguide core/clad list really

should be expanded to include Ge and SiGeSn and β -SiC as the top MIR-waveguiding core layer; i.e., SiGeSnOI, SiGeSnOS, SiGeSnON, SiCOI, SiCOS and SiCON. In addition, the group IV MIR waveguide core strip can be grown directly upon a bulk Si substrate as in the recent experimental development of Ge on Si^{31,32}. Another important approach is to “undercut” the group IV core via etching to leave an air pocket under the core^{24,33,34}, namely the “suspended” Si, Ge, SiGeSn, and porous-Si waveguides. It’s fascinating that Ge has uses in free-space acousto-optics³⁵ as well as in guiding light.

6.1 Group IV plasmonics

The new discipline of “Group IV plasmonics”^{1,36,37,38} enters into the MIR waveguiding picture as composite channel waveguides whose cross-section dimensions are smaller than those set by the optical diffraction limit, such as the “gap plasmon” mode waveguide³⁹. For active EO MIR waveguided modulators and switches, I propose a scaled-up version of the 4-layer waveguide-strip device³⁶ comprised of copper, SiO₂, indium-tin oxide and p-silicon. Waveguiding in the so-called hybrid-mode uses MIR SPP guidance at conductor/dielectric interface(s) in combination with internal MIR reflection in the dielectric strip³⁷. We propose that the “dielectric” is intrinsic Si or Ge or SiGeSn, and the conductor is an ultrathin $\lambda/100$ ribbon of silicide, germanicide, doped Si or doped Ge buried within the dielectric. The buried ribbon⁴¹ is one of several conductor/dielectric plasmonic waveguide channels whose loss decreases with increasing IR wavelength.

7. ON-CHIP SPECTROMETERS AND REFRACTOMETERS

7.1 Transitioning from 1.31 and 1.55 μm to the 2-to-5 μm wavelengths

Creating the MIR chips is a worthy enterprise that will take effort and ingenuity. That creation requires uncovering new physics, employing some “unfamiliar” materials, and designing new structures. Because successful integrated sensors already exist in the 1.55 μm region⁴², the path to a viable MIR sensor chip is often to scale-up the waveguide dimensions of a telecom chip and to modify its configuration for MIR operation. A thesis of this paper is that scaling-and-modifying telecom chips is a key technique for the transition to MIR chips. Several examples are given below.

7.2 The various types of spectrometers

A variety of refractometers and spectrometers offer promise for on-chip MIR chem bio sensing. A refractometer usually targets the behavior of the analyte at a particular wavelength that is emblematic of those molecules²⁵, while the spectrometer, by definition, covers a wavelength range. A refractometer that is resonant at the desired wavelength is quite useful, and a new periodically tuned electro-optic resonator (PTEOR) technique⁴³ offers a significant advance in refractometer sensitivity, perhaps allowing parts-per-billion detection.

There is “room for invention” of chip spectrometers in the categories of Raman, surface enhanced Raman, plasmonic ATR^{44,45,46,47}, finite Fourier transform, fluorescence, infrared absorption⁴⁸, photo-thermal, and photo-acoustic. This is an opportunity and a challenge. To detect a particular chem-bio agent, the different spectroscopic approaches can be traded off against each other to find the best one. As to sensing the physical quantities of temperature, pressure, velocity, acceleration, rotation (in a gyroscope), etc., such sensing is surely feasible at MIR but the advantage of doing so there rather than at shorter wavelengths is not clear; whereas the motivation is strong for seeking chem-bio “signatures” at MIR because that is where most molecules exhibit their fundamental vibrations and transitions. There are literally dozens of spectrometer designs that could be implemented, and here the reader is directed to reports in the photonics literature of experimental sensors operating at 1.55 μm . Those results highlight chips that could be reconfigured for MIR application. In the next two subsections, I shall give specific proposals for two new kinds of MIR chip spectrometers.

7.3 Ge blackbody source for spectrometers

For infrared absorption spectroscopy, it is sometimes proposed that a tunable laser diode could be sited on chip to scan across the desired spectrum. This is difficult to achieve. An alternative is to “dissect” a spectrally broad source such as a superluminescent LED. There is a second broad-source idea—blackbody (BB) radiation— not exploited yet on chip—and I shall set forth here a possible waveguided blackbody. Conventionally, the BB emitter requires a large temperature rise above 500K. However, there is a clever way to minimize the heating requirement by optical pumping of a locally heated

Si or Ge area as demonstrated by Malyutenko and Bogatyrentko⁴⁹. I have modified their free-space Ge configuration by proposing a Ge waveguided BB source with a microstrip heater (localized at the input) and an off-chip 1.55 μm pump that provides wavelength down-conversion over a 70 μm Ge MIR nanowire segment. Thus the wire emits 2 to 14 μm radiation along the intrinsic undoped waveguide. That emission is prefiltered to a 3-to-5 μm band before it enters the serpentine slotted waveguide immersed in the analyte's microfluid area. Then the waveguided molecular absorption spectrum is sent to a discrete Fourier Transform analyzer comprised of an N-fold waveguided array of unbalanced Mach-Zehnder interferometers^{50,51} that feeds a photodiode array linked to an on-chip transform computer. This scenario is illustrated in Fig. 4. Only 4 of N spatial heterodynes are shown.

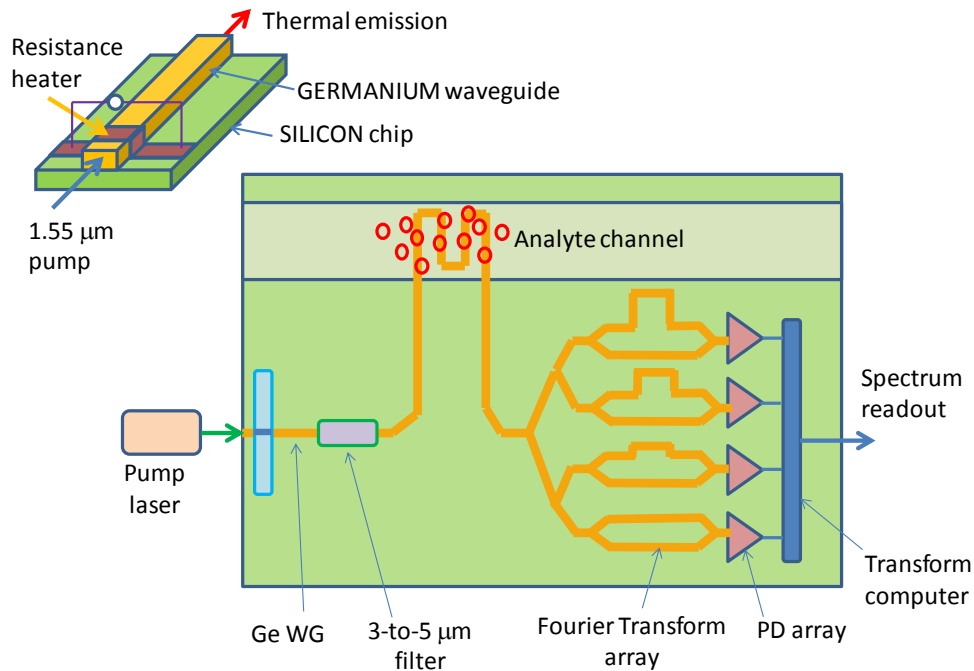


Figure 4. Perspective view of Si-based Ge blackbody waveguided emitter and top view of waveguided spectrometer-on-a-chip with waveguided Fourier-Transform analysis of the analyte's absorption spectrum.

7.4 Frequency comb source for spectrometers

The unusual but valuable MIR frequency-comb source^{52,53} employs cascaded phase-matched four wave mixing in nonlinear-optical Si or Ge channel waveguides (nano wires). These wires enable an OPO configured to generate an wide-band infrared frequency-comb of emission with its spectrum centered on the MIR wavelength of the pump laser. The pump wavelength is $> 2.1 \mu\text{m}$ for Si and $> 3.6 \mu\text{m}$ for Ge in order to avoid two photon absorption in the NLO waveguide structure. Building upon the work of Foster *et al*⁵⁴, I suggest in Figure 5 a Si or Ge MIR microring that is resonant at the pump and signal and idler wavelengths—with the comb output arising from the bus waveguide side-coupled to the ring. The ring must have very high Q, the ring must be dispersion engineered to have a broad anomalous group velocity dispersion near the pump wavelength for efficient parametric FWM, and the spectral line spacings within the comb should be easy-to-detect microwave frequencies in the GHz range. As with the above BB, the comb source relies upon a rather strong off-chip pump laser, which can be a semiconductor diode laser. (A totally on-chip source would be ideal, especially if the source is inexpensive and the chip is intended to be “disposable”. However the physical size and heat-dissipation requirements of some sources may keep those sources separate from the chip but linked to it by a specialty fiber). The comb of closely spaced MIR spectral lines is waveguided into the molecular interaction area (microfluid channel) where molecular absorption reduces the amplitude of some spikes. Thereafter the modified spectral spikes travel to a very fast MIR photodiode. A tapped-off portion of the original single-frequency pump is sent to the same PD whose nonlinearity acts as a coherent infrared mixer, thereby creating difference-frequency generation (interference) between the pump and the lines⁵⁵. That group of microwave “beat signals” is sent an off-chip microwave spectrum analyzer that constructs the (discretely) measured MIR spectrum of the target species.

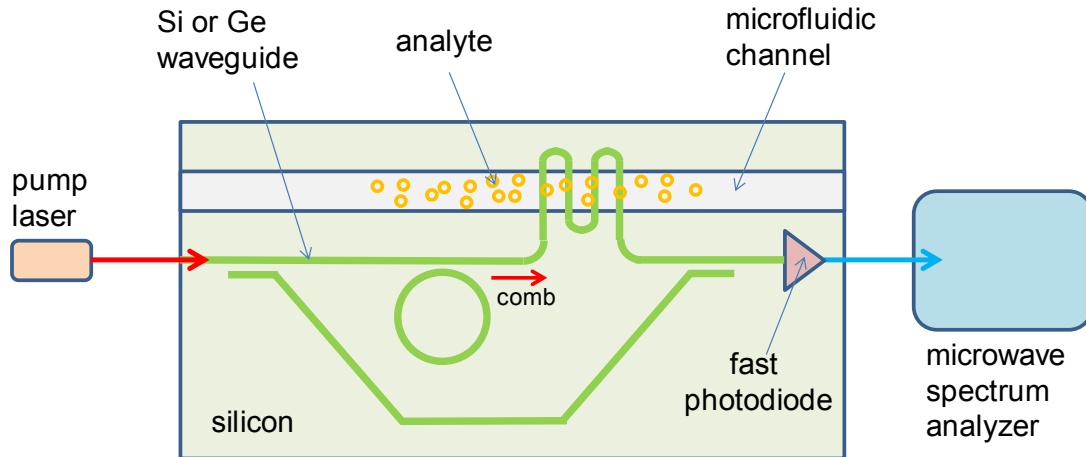


Figure 5. Plan view of frequency-comb on-chip MIR spectrometer featuring interference of the single-frequency pump with the modified comb lines (microwave beat signals).

7.5 Refractometers

There are excellent possibilities here. If we focus for a moment on plasmonics, the attenuated total reflection (ATR) is in essence a very sensitive “free space” refractometer, and the task here is to modify this structure into a guided-wave sensor--which has been done recently⁵⁶. For example, a bio-sensing refractometer employed a micro-ring gap-plasmon waveguide resonator⁵⁷ that looks promising for MIR implementation. All-semiconductor (dielectric) refractometers are important too. The silicon nanobeam (NB) resonator which contains a tapered 1D PhC hole-or-slot array looks attractive for MIR refractometry⁵⁸.

7.6 Detection of trace gases

This MIR sensor application includes medical diagnosis as well as detecting trace amounts of carbon dioxide, carbon monoxide, methane, sulfur dioxide, etc. The medical sensing refers to (1) detecting trace amounts of glucose in exhaled breath (a breathalyzer) for noninvasive diabetes monitoring and (2) detecting alkalinity in exhaled breath for asthma applications. Trace amounts present a significant challenge. In the past, concentration of gas has been necessary using large free-space gas cell, but there is evidence that traces can be found on-chip without a concentrator. For example, simulations by Passaro *et al*⁵⁹ at $\lambda = 3.39 \mu\text{m}$ indicate that gas infused into the slot of an SOI group IV waveguide-wire structures changes the cladding index and the quasi-TE mode effective index with respect to an air cladding. Assuming an 80 pm detectable wavelength shift in a 100-nm-width slotted resonator, they say that 3.6×10^{-5} refractive index units is the limit of detection. This can be improved with the aforementioned PTEOR. The Si NB cavity can be slotted for a similar ultrasensitive PTEOR refractometer⁵⁷. To attain very high sensitivity for ethane and methane detection, the Vernier effect using two cascaded ring resonators was demonstrated⁶⁰. Another example is the highly innovative design study of Lin *et al*⁶¹ who employ a chalcogenide glass layer on Si that is fashioned into a PhC cavity doubly resonant at the pump and MIR signal wavelengths. They estimate that their photo thermal approach will yield single molecule detection (!) at MIR.

8. HYBRID INTEGRATION OF ON-CHIP SOURCES, DETECTORS, MODULATORS

8.1 Active III-V devices hybrid-integrated on Si or Ge

Hybrids are definitely the short-term solution to MIR on-chip “actives.” The primary devices are lasers, photodetectors⁶², electrooptical modulators^{62,63,64}, MIR amplifiers and resonant or non-resonant electro optical routing switches. Both interband cascade lasers⁶⁵ (ICLs) and quantum cascade lasers⁶⁶ (QCLs) are excellent candidates because of their MIR room-temperature operation. The principle approach is thin-film BCB bonding of the III-V to the exposed top surface of the group IV waveguide network to achieve vertical, evanescent-wave coupling. For the various III-V actives, I

propose that the bottom doped-contact-layer of the device should be thinned for such coupling. Thus modified, commercial ICLs and QCLs could be bonded. As an alternative, I would suggest that the Ge diffraction grating present on some III-V DFB ICL devices be bonded upside down on a Ge waveguide⁶⁷. Another hybrid approach is to mount an edge-emitting/detecting III-V active “die” in a trench etched at one end of a group IV waveguide for end-fire coupling into the guide⁶⁸. Membrane transfer and bonding is also a fine approach. In his many papers on semiconductor nanomembranes (SNMs), Professor Z. Q. Ma has shown that a given SNM can be bonded successfully to essentially “any” substrate-- an “anything on anything” situation that does not require lattice matching, a technique very applicable to MIR devices^{69,70,71,72}. Finally, an important MIR technique is hetero-epitaxial growth of III-V layered active structures directly upon group IV, and here lattice matching (or near matching) is demanded. If we constrain this problem further by saying that the III-V actives should have a direct bandgap in the 0.25 to 0.62 eV range, this indicates that the alloys are in the InGaAsSb or InGaAsP families, and that the III-V lattice parameter must be close to 0.6 nm. If the waveguide is Ge, then one or two relaxed buffer layers of SiGeSn must be grown on Ge to reach the 0.6 nm template. This VS requirement places the burden of proof on SiGeSn rather than on the more mature InGaAsSb. In other words, lattice matched MIR hybrids can be grown if and when the feasibility of SiGeSn having large fractions of Sn and Ge is proved.

8.2 II-VI and lead salt semiconductors, chalcogenides and rare earth ions for hybrid devices

Heterogeneous integration on Si is also feasible with these materials. For making MIR devices, the rare earth ions would go *into* silicon, while the II-VI/lead-salt semiconductors and the chalcogenide glasses would go *onto* silicon. Specifically, we note that Tm³⁺ in Si shows promise⁷³ as an optically pumped (and eventually electrically pumped) 2.04 μm emitter at 300K. Only the alloys offering room temperature operation for 2 to 3 μm are considered here. That’s why PbS and the CdPbS alloys are examples of active layers for MIR lead-salt emitter/sensor structures⁷⁴. The bonding techniques discussed above would work for II-VI/Si hybrids. For CdPbS epitaxy on Si, relaxed buffers are needed to match the lead salt 0.59-nm zincblende lattice. Deposition of arsenic selenide glass and lead salt materials in the amorphous state on Si has device value too. Quantum dots within an active layer, such as Ge or InGaAs QDs, can enable better light emission and photodetection⁷⁵. However, we do not have space here to cover those devices. The chalcogenide glasses, which are highly transmission MIR materials, can be deposited readily on silicon to form MIR waveguides⁷⁶ and related structures for on-chip chem-bio sensors as discussed above in Section 7.6.

9. MONOLITHIC INTEGRATED SiGeSn HETEROSTRUCTURE LASERS AND DETECTORS

9.1 Hetero-devices of GeSn and SiGeSn

At several laboratories around the world, research continues on the growth of SiGeSn via CVD and MBE. Experimental SiGeSn epitaxy on Si and Ge continues to gain credibility and momentum (although these are “early days” by comparison to III-V maturity). Generally, the motivation is to attain *totally monolithic* integration of active and passive heterodevices on Si and Ge-- integration of the entire group in a factory⁷⁷.

The empirical pseudopotential theory predicts a wide range of useful Si-based SiGeSn MIR materials and heterostructures⁷⁸. This first-principles promise, however, collides with real-world epitaxial growth issues about the miscibility and the thermodynamic stability of these ternary materials when the fraction of Sn is “high”. Some clever meta-stable growth techniques may have to be developed in order to actualize the SiGeSn/(SiGeSn)’ MIR multiple-quantum-well (MQW) devices highlighted in Ref. 79. With this caveat, let’s look at potential MIR devices that rely on band-to-band transitions (such as dual heterostructures or DH) and intersubband transitions (the MQW structures). DH detector prospects are excellent, but the DH laser diode suffers from Auger recombination that would necessitate cooling the LD for reasonable thresholds⁸⁰. However the MQW LD appears to be indeed a viable room-temperature approach for amplification and lasing in the 1.9 to 2.5 μm range⁷⁹. The PIN MQW structures (not yet demonstrated!) have versatility for several photonic tasks including modulation and detection. Regarding actual experiments, work in Taiwan⁸¹ and Europe on GeSn light emitting diodes is progressing nicely⁸². And there are impressive results on the 2.2 μm response of Ge/GeSn/Ge MQW photodiodes⁸³. The “all group IV” QCL prospects are better at wavelengths longer than 5 μm than at MIR because $\lambda < 5 \mu\text{m}$ requires deep quantum wells that introduce considerable strain. The “all group IV” ICL requires type II band alignments that may not be available in this materials system.

Efficient, low-energy MIR modulation (both electro-refraction and electro-absorption) as well as electro-optical MIR spatial routing (switching) is guaranteed by the physics of Si and Ge and GeSn and SiGeSn. The main techniques are the free-carrier plasma dispersion effect (FCE), the Franz-Keldysh effect in “bulk” crystals (FKE), and the quantum-confined Stark effect (QCSE) in MQW waveguides. Progress in theory and experiment has been made recently in (1) new understanding of the FCE in Si and SiGe over the 2 to 14 μm wavelength range^{84,85,86}, (2) estimates of the MIR FKE⁸⁷ in alloys of GeSn containing up to 12 % Sn, and (3) prediction of GeSn MIR QCSE in GeSn/SiGeSn MQWs.

10. NONLINEAR OPTICS APPLIED TO MIR SYSTEM-CHIPS

The nonlinear optical (NLO) properties of group IV waveguide materials have at least three uses in MIR system chips: (1) efficient up-and-down wavelength conversion for chip transceivers, (2) creation of an on-chip MIR frequency-comb source, (3) on-chip supercontinuum generation⁸⁸. All of these require a rather intense *pump laser* or laser diode. At present, that laser would be off chip (e.g., a Tm-based fiber laser), although future development would put an LD on the chip. These three applications rely upon the strong third-order NLO effects in Si, SiGe, Ge, and SiGeSn as applied to phase-matched four-wave mixing (FWM) in dispersion-engineered²⁹ waveguides. In the case of SiGeSn, the composition must be chosen for transparency at pump, signal and idler wavelengths. I have co-authored reviews of the third-order NLO coefficients of Si, SiGe and Ge over the MIR/LWIR ranges^{89,90} which show that Ge has the strongest response. As mentioned above in Section 7.4, the pump wavelength must be selected to avoid TPA. GeSn is “more nonlinear” than Ge but has a narrower fundamental bandgap. It should be noted that

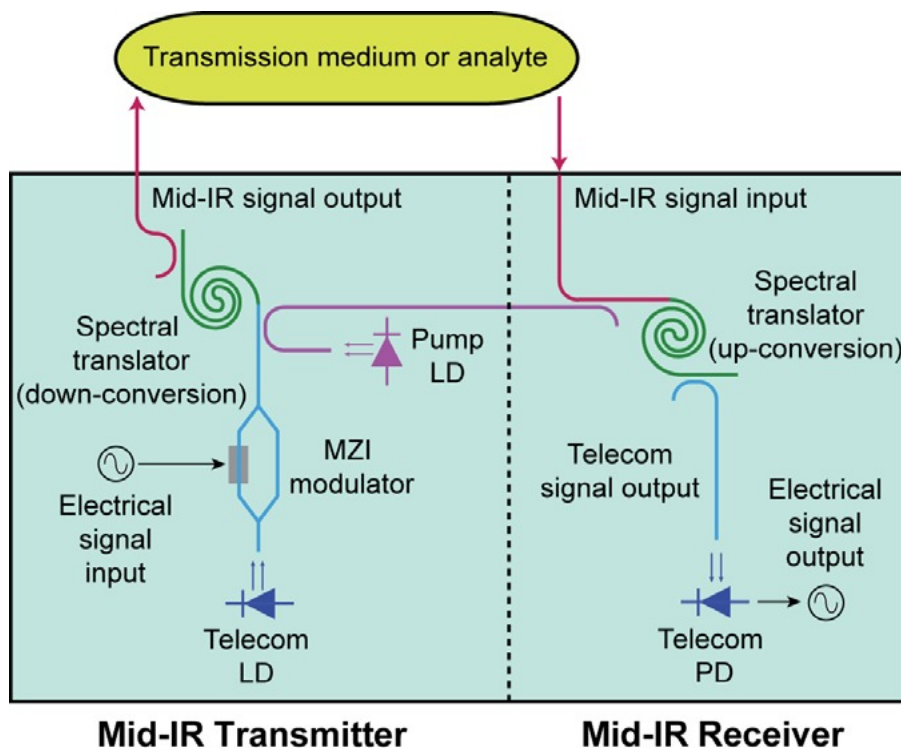


Figure 6. Proposed one-chip SOI MIR transceiver using FWM as well as a telecom LD and a telecom PD.

all of the above group IV waveguides, the elements and the alloys, can exhibit a practical second-order NLO response if (and only if) the waveguide is inhomogeneously strained by a dielectric film such as Si_3N_4 deposited on the waveguide’s exposed top surfaces. This has been shown for Si⁹¹ and should, in my opinion, work well for the other group IV materials. Three wave mixing (TWM) characterizes the second order materials⁹¹ and TWM will produce the same chip applications⁹² listed above for FWM. I believe that amorphous Si, SiGe and Ge can offer useful NLO effects. It is somewhat surprising that *a*-Si:H has a strong third-order effect as proven by experiments¹⁴. If the amorphous

hydrogenated Si waveguide is capped or shielded from visible light to avoid the Stabler-Wronski effect, I predict that this NLO waveguide will be stable and practical.

Groups at IBM, Columbia University and Gent University have measured fairly efficient frequency conversion in a 2-cm length of dispersion-engineered SOI nanowire waveguide coiled into a sub-mm spiral⁹³. They have proposed a wavelength-converting transceiver chip that is worthy of further investigation. The duplex chip is illustrated in Figure 6. One on-chip LD pumps both Si spirals, each of which is coupled to a MIR fiber. These fibers travel to and from a remote location for a communications link or for sensing of an analyte. MIR- to-telecom and telecom-to-MIR conversions take place simultaneously on the same SOI chip. The beauty of the chip is that it uses only well-known *telecom* components on the chip to get fairly efficient MIR emission as well as high-signal-to-noise detection of weak MIR. As an alternative to fiber coupling, the chip can couple to free space if desired.

An interesting footnote on FWM in a crystal Si nano wire pertains to frequency down-conversion of a 4.3 μm pump. If the “suspended” WG is clad below and above by air, the MIR pump can be converted to THz with 1 % efficiency⁹⁴.

11. CONCLUSION

We have described a host of possibilities for group IV MIR system-on-a-chip techniques and applications. This manuscript was written in January of 2013 about four weeks prior to the February 2-7 SPIE Photonics West OPTO conferences. From an examination of the advance program of OPTO, it is clear that the topics covered in this paper are being investigated vigorously in the photonics community as exemplified by 2013 OPTO papers 8627-18, 8631-64, 8631-34, 8631-9, 8627-36, 8631-39 and 8627-36.

ACKNOWLEDGEMENT

The author wishes to thank the Air Force Office of Scientific Research, Dr. Gernot Pomrenke, Program Manager, for sponsoring this work under Grant FA9550-10-1-0417.

REFERENCES

- [1] Soref, R., “Towards Silicon-based Longwave Integrated Optoelectronics (LIO), SPIE Proceedings 6898 (2008); invited paper 6898-5, SPIE Photonics West, Silicon Photonics III Conference, San Jose, CA (21 Jan 2008).
- [2] Hendrickson, J., Guo, J., Zhang, B., Buchwald, W. and Soref, R., “Wideband perfect light absorber at midwave infrared using multiplexed metal structures,” *Optics Letters* 37, 371-373 (2012).
- [3] Soref, R. A., “Silicon-based optoelectronics,” *Proceedings of the IEEE* 81, 1687-1706 (1993).
- [4] Sherwood-Droz, N. and Lipson, M., “Scaleable 3D dense integration of photonics on bulk silicon,” *Optics Express* 19(18), 17758-17765 (2011).
- [5] Soref, R., “Reconfigurable integrated optoelectronics,” *Advances in Opto-Electronics*, article ID 627802, published online at www.hindawi.com (May 2011).
- [6] Soref, R. A., Cho, S. Y., Buchwald, W. and Cleary, J., “Silicon plasmonic waveguides,” Chapter in 2 in [*Silicon Photonics for Telecommunications and Biomedicine*], Fathpour and Jalali, Editors, CRC Press, Boca Raton and London 52-76 (2012).
- [7] Mashanovich, G. Milosevic, M. M., Nedeljkovic, M., Chong, H. M. and Soref, R., “Mid-infrared silicon photonics for sensing applications” paper L2.3 (invited) *Materials Research Society Spring Meeting, Symposium L*, San Francisco, CA (10 April 2012).
- [8] Mashanovich, G. Z., Nedeljkovic, M., Milosevic, M. M., Hu, Gardes, F. Y. Thomson, D. J., Ben Masaud, T., Jaberansary, E., Chong, H. M. H., Soref, R. and Reed, G. T., “Group IV photonic devices for the mid-infrared,” paper 8431-12 (invited), *SPIE Photonics Europe Conference*, Brussels, Belgium (17 April 2012).
- [9] Novoselov, K. S., Falko, V. I., Colombo, L., Gellert, P. R., Schwab, M. G. and Kim, K., “A roadmap for graphene,” *Nature* 490, 192-200 (11 Oct 2012).
- [10] Koester, S. J. and Li, M., “High-speed waveguide-coupled graphene-on-graphene optical modulators,” *Applied Physics Letters* 100(17), 171107 (2012).

- [11] Gu, T., Petrone, N., McMillan, J. F., van der Zande, A., Yu, M., Lo, G. Q., Kwong, D. L., Hone, J. and Wong, C. W., "Regenerative oscillation and four-wave mixing in graphene optoelectronics," *Nature Photonics* 6, 554-559 (August 2012).
- [12] Bechstedt, F., Matthes, L., Gori, P. and Pulci, O., "Infrared absorbance of silicene and germanene," *Applied Physics Letters* 100, 261906 (2012).
- [13] Checoury, X., Neel, D., Boucard, P., Gesset, C. and Girard, H., "Nanocrystalline diamond photonics platform with high quality factor photonic crystal cavities," *Applied Physics Letters* 101, 171115 (2012).
- [14] Narayanan, K. and Preble, S. F., "Optical nonlinearities in hydrogenated-amorphous silicon waveguides," *Optics Express* 18(9), 13529-13535 (2011).
- [15] Whistey, M. A., "Direct bandgap low-carbon GeC alloys," unpublished memorandum (2012).
- [16] Virgilio, M., Pizzi, G. and Grosso, G., "Optical gain in short period Si/Ge superlattice on [001]-SiGe substrate," *Journal of Applied Physics* 110, 083105 (2011).
- [17] Li, H., Anugrah, Y., Koester, S. J. and Li, M., "Optical absorption in graphene integrated on silicon waveguides," *arxiv.org*, paper 1205.4050 (2010).
- [18] Labeye, P., et al, "Integrated optics beam combiner at 2.2 μm for astronomical interferometers," *Conference on Lasers and Electrooptics EUROPE/EQEC*, article 594682 (2011).
- [19] Duc Nguyen, V., Weiss, N., Beeker, W., Hoekman, M., Leinse, A., Heidman, R. G., van Leewen, T. G. and Kalkman, J., "Integrated-optics-based swept-source optical coherence tomography," *Optics Letters* 37, 4820-4822 (2012).
- [20] Ong, J. R., Davanco, M., Shehata, A. B., Tosi, A., Agha, A., Assefa, S., Xia, F., Vlasov, Y. A., Green, W. J. M., Srinivasan, K. and Mookherjee, S., "Heralded single photons from a silicon nanophotonic chip," *Conference on Lasers and Electrooptics*, paper CTh3M.6, San Jose, CA (6 May 2012).
- [21] Soref, R. A., "Semiconductor photonic nano-communication link method," US Patent 7,907,848 (15 Mar 2011).
- [22] Ko, M., Youn, J. S., Lee, M. J., Choi, K. C., Rucker, H. and Choi, W. Y., "Silicon photonic- wireless interface IC for 60-GHz wireless link," *IEEE Photonics Technology Letters* 24, 1112-1117 (2012).
- [23] Genalyte-and-IMEC press release http://www2.imec.be/be_en/press/imec-news/imecgenalyte.html
- [24] Soref, R., Emelett, S. J. and Buchwald, W. R., "Silicon waveguided components for the long-wave infrared region," *Journal of Optics A (Pure and Applied Optics)* 8, 840-848 (2006).
- [25] Soref, R., "Mid-infrared photonics in silicon and germanium," (Invited Commentary) *Nature Photonics* 4, 495-497 (August 2010).
- [26] Soref, R., "Mid-infrared silicon photonic integrated circuits," (invited) OSA Topical Conference on Integrated Photonics Research, Toronto, Canada (13 June 2011).
- [27] Mashanovich, G., Nedeljkovic, M., Milosevic, M., Ben Masaud, T., Jaberansary, E., Reimer, C., Stothard, D., Krauss, T. F., Chong, H. and Reed, G. T., "SOI mid-infrared photonics for the 3-4 μm wavelength range," *Frontiers in Optics Conference*, Rochester, NY (14 Oct 2012).
- [28] Cheng, Z., Chen, X., Wong, C. Y., Xu, K., Fung, C. K. Y., Chen, Y. M. and Tsang, H. K., "Mid-infrared grating couplers for silicon-on-sapphire waveguides," *IEEE Photonics Journal* 4(1), 104-113 (2012).
- [29] Yang, Y., Li, Z., Hao, H., Beausoleil, R. G. and Willner, A. E., "Silicon-on-nitride waveguide with ultralow dispersion over an octave-spanning mid-infrared wavelength range," *IEEE Photonics Journal* 4(1), 126-132 (2012).
- [30] Reimer, C., Nedeljkovic, M., Stothard, D. J. M., Esnault, M. O. S., Reardon, C., O'Faolain, L., Dunn, M., Mashanovich, G. Z. and Krauss, T. F., "Mid-infrared photonic crystal waveguides in silicon," *Optics Express* 20, 29361-29368 (2012).
- [31] Chang, Y. C., Paeder, V., Hvozdar, L., Hartmann, J. M., and Herzig, H. P., "Low-loss germanium strip waveguides on silicon for the mid-infrared," *Optics Letters* 37, 2883-2885 (2012).
- [32] Chang, Y. C., Wagli, P., Paeder, V., Homsy, A., Hvozdar, L., van der Wal, P., Di Francesco, J., de Rooij, N. F. and Herzig, H. P., "Cocaine detection by a mid-infrared waveguide integrated with a microfluidic chip," *Lab on a Chip* 12, 3020-3023 (2012).
- [33] Wei, Y., Li, G., Hao, Y., Li, Y., Yang, J., Wang, M. and Jiang, X., "Long-wave infrared 1 x 2 MMI based on air-gap beneath silicon rib waveguides," *Optics Express*, 19, 15803-15809 (2011).
- [34] Cheng, Z., Chen, X., Wong, C. Y., Xu, K. and Tsang, H. K., "Mid-infrared suspended membrane waveguide and ring resonator on silicon-on-insulator," *IEEE Photonics Journal* 4(5), 1510-1519 (2012).
- [35] Nite, J. M., Cyran, J. D. and Krammel, A. T., "Active Bragg angle compensation for shaping ultrafast mid-infrared pulses," *Optics Express* 20, 23912-23930 (2012).

- [36] Soref, R. A., Peale, R. and Buchwald, W., "Longwave Plasmonics on doped silicon and silicides," *Optics Express*, 16, 6507-6514 (2008).
- [37] Soref, R. A., Cho, S. Y. Buchwald, W. R. and Peale, R. E., "Silicon plasmonic waveguides for infrared and Terahertz applications," (invited) paper PDS-25-4-1, SPIE Photonics North, Quebec City, Canada (25 May 2009).
- [38] Soref, R., Hendrickson, J. and Cleary, J. W., "Mid- to long-wavelength infrared plasmonic-photonics using heavily doped n-Ge/Ge and n-GeSn/GeSn heterostructures," *Optics Express* 20, 3814-3824 (2012).
- [39] Avrutsky, I., Soref, R. and Buchwald, W., "Sub-wavelength plasmonic modes in a conductor-gap-dielectric system with a nanoscale gap," *Optics Express* 18, 348-363 (2010).
- [40] Sorger, V. J., Lanzillotti-Kimura, N. D., Ma, R. M. and Zhang, X. "Ultra-compact silicon nanophotonic modulator with broadband response," *Nanophotonics* 1(1), 17-22 (2012).
- [41] Cho, S. Y. and R. A. Soref, R. A. "Low-loss silicide/silicon plasmonic ribbon waveguides for mid- and far-infrared applications," *Optics Letters* 43, 1759-1761 (2009).
- [42] Song, J., Zhou, X., Li, Y. and Li, X., "On-chip spectrometer with a circular-hole defect for optical sensing applications," *Optics Express* 20, 19226-19231 (2012).
- [43] Qiu, C., Chen, J. and Xu, Q., "Ultraprecise measurement of resonance shift for sensing applications," *Optics Express* 37, 5012-2015 (2012).
- [44] G. Mehdi, J. W. Cleary, R. E. Peale, G. D. Boreman, I. Oladeji, R. Soref, S. Wentzell, and W.R. Buchwald "Surface plasmon resonance biosensor based on characteristic biomolecular vibrations," 13th International Conference on Vibrations at Surfaces (VAS13), University of Central Florida, Orlando FL, March 10-13 (2010).
- [45] Cleary, J. W., Peale, R. E., Shelton, D. J., Boreman, G. D., Smith, C. W., Ishigami, M., Soref, R., Drehman, A. and Buchwald, W. R., "IR permittivities for silicides and doped silicon," *Journal of the Optical Society of America B* 27, 730-734 (2010).
- [46] M. Shahzad, G. Medhi, R. E. Peale, W. R. Buchwald, J. W. Cleary, R. Soref, G. D. Boreman and O. Edwards, "Infrared surface plasmons on heavily doped silicon," *Journal of Applied Physics* 110, 123105 (2011).
- [47] Peale, R. E., Cleary, J. W., Shelton, D., Boreman, G., Soref, R. and Buchwald, W., "Silicides for infrared surface Plasmon resonance biosensors", *Proceedings of the Materials Research Society* 1133 Symposium AA, paper 10-03 Fall MRS meeting, Boston, MA, (1 Dec 2008).
- [48] Hassanzadeh, S., Ebanili-Heidari, A., and Kamutsch, "Design of an on-chip absorption spectrometer using optofluidic slotted photonic crystal structures," *IEEE Photonics Journal* 4, 1484-1494 (Oct 2012).
- [49] Malyutenko, V. K. and Bogatyrenko, V. V., "Light down-conversion with over 100 % external quantum efficiency in bulk germanium," *Applied Physics Letters* 101, 081111 (2012).
- [50] Cheben, P., Florjanczyk, M., Bock, P., Ramos, C. A., Lamontagne, B., Bogdanov, A., Janz, S. Xu, D.-X., Vachon, M., Scott, A. Ortega-Monux, A., Molina-Fernandez, I., Solheim B. and Sinclair, K., "Recent advances in Fourier-Transform waveguide spectrometers", paper TuA.2.1, 13th Intl. Conf. on Transparent Optical Networks, Stockholm (2011).
- [51] Florjanczyk, M., Cheben, P., Janz, S., Scott, A., Solheim, B. and Xu, D.-X., "Multiaperture planar waveguide spectrometer formed by arrayed Mach-Zehnder interferometers," *Optics Express* 15(26), 18176-18189 (2008).
- [52] Schliesser, A., Picque, N., and Hansch, T. W., "Mid-infrared frequency combs," *Nature Photonics* 6, 440-449 (July 2012).
- [53] Saha, K., Okawachi, Y., Levy, J. W., Lau, R. K., Luke, K., Foster, M. A., Lipson, M. and Gaeta, A. L., "Broadband parametric frequency comb generation with a 1- μ m pump source," *Optics Express*, 20, 26395-26941 (2012).
- [54] Foster, M. A., Levy, J. S., Kuzucu, O., Saha, K., Lipson, M. and Gaeta, A. L., "Silicon-based monolithic optical frequency comb source," *Optics Express* 19, 1433-14239 (2011).
- [55] Urabe, K. and Sakai, O., "Absorption spectroscopy using interference between optical frequency comb and single-wavelength laser," *Applied Physics Letters* 101, 051105 (2012).
- [56] Khalizadeh, F., Fredericksen, C., Buchwald, W., Cleary, J., Smith, E., Rezadad, I. Nath, J., Figueiredo, P., Shahzad, M., Boroumand, J., Yesiltas, M., Medhi, G., Davis, A. and Peale, R., "Planar integrated plasmonic mid-IR spectrometer," paper DD14.05, presented at the Materials Research Society Fall Meeting, Boston, MA (2012).
- [57] Zhou, L., Sun, X., Li, X. and Chen, J., "Miniature microring resonator sensor based on a hybrid plasmonic waveguide," *Sensors* 11, 6856-6867 (2011).
- [58] Hendrickson, J., Sweet, J. and Soref, R., "Silicon nanobeam electro-optical modulators" unpublished memorandum (2012).

- [59] Passaro, V. M. N., Troia, B. and De Leonardis, F., "Group IV photonic slot structures for highly efficient gas sensing in mid-IR," 2nd Intl. Conf. on Sensor Device Technologies and Applications, Nice, France (21 Aug 2011). ISBN: 978-1-61208-145-8
- [60] Passaro, V. M. N., De Tullio, C., Troia, B., La Notte, M. Giannoccaro, G., and De Leonardis, F., "Recent advances in integrated photonic sensors," *Sensors* 12, 15558-15598 (2012).
- [61] Lin, H., Zou, Y. and Hu, J., "Double resonance 1-D glass-on-silicon photonic crystal cavities for single-molecule mid-infrared photothermal spectroscopy; theory and design," poster paper WP20, IEEE 9th Intl. Conf. on Group IV Photonics, San Diego (30 August 2012).
- [62] Hattasan, N., Cerutti, L., Rodriguez, J. B., Tournie, E., Van Thourhout, D. and Roelkens, G., "Heterogeneous GaSb/SOI mid-infrared photonic integrated circuits for spectroscopic applications," SPIE online proceedings, <http://dx.doi.org/10.1117/12.874659>.
- [63] Tang, Y., Peters, J. D. and Bowers, J. E., "Energy-efficient hybrid silicon electroabsorption modulator for 40-Gb/s 1-V uncooled operation," *IEEE Photonics Technology Letters* 24(19), 1689-1692 (2012).
- [64] L. Liu, J. Van Campenhout, G. Roelkens, R. A. Soref, D. Van Thourhout, P. Rojo-Romeo, P. Regreny, C. Seassal, J. M. Fedeli and R. Baets, "Carrier-injection-based electro-optic modulator on silicon-on-insulator with a heterogeneously integrated III-V microdisk cavity," *Optics Letters* 33, 2518-2520 (2008).
- [65] Bewley, W. W., Canedy, C. L., Kim, C. S., Kim, M., Merritt, C. D., Abell, J., Vurgaftman, I. and Meyer, J. R., "High-power room-temperature continuous-wave mid-infrared interband cascade lasers," *Optics Express* 20, 20994-20901 (2012).
- [66] Yao, Y., Hoffman, A. J. and Gmachl, C. F., "Mid-infrared quantum cascade lasers," *Nature Photonics*, 6, 432-439 (2012).
- [67] Kim, C. S., Kim, M., Abell, J., Bewley, W. W., Merritt, C. D., Canedy, C. L., Vurgaftman, I. and Meyer, J. R., "Mid-infrared distributed-feedback interband cascade lasers with continuous-wave single-mode emission to 80 °C," *Applied Physics Letters*, 101, 061104 (2012).
- [68] Famenini, S., "Integration of edge-emitting laser diodes with dielectric waveguides on silicon," *IEEE Photonics Technology Letters* 24(20), 1849-1851 (2012).
- [69] Yang, H., Zhao, D., Chuwongin, S., Seo, J-H., Yang, W., Shuai, Y., Berggren, J., Hammar, A., Ma, J. and Zhou, W., "Transfer-printed stacked nanomembrane lasers on silicon," *Nature Photonics* 6, 615-620 (July 2012).
- [70] Shuai, Y., Zhao, D., Zhou, W., Ma, Z., Medhi, G., Peale, R., Buchwald, W. and Soref, R., "Fano resonance membrane reflectors from mid-infrared to far-infrared", IEEE Photonics Society Annual Meeting, paper ThN3, Arlington, VA (9 Oct 2011).
- [71] Zhou, W., Ma, Z., Yang, W., Chuwongin, S., Shuai, Y. C., Seo, J. H., Zhao, D., Yang, H. and Soref, R., "Semiconductor nanomembranes for integrated and flexible photonics," (invited) Digest of Papers, Information Photonics 2011 Conference, Ottawa, Canada (18 May 2011).
- [72] Kiefer, A. M., Paskiewicz, D. M., Clausen, A. M., Buchwald, W. R., Soref, R. A. and Lagally, M. G., "Si/Ge junctions formed by nanomembrane bonding", *ACS Nano* (19 Jan 2011). DOI: 10.1021/nn103149c
- [73] Murray, M. T., Fernandez, T. T., Richards, B., Jose, G. and Jha, A., "Tm³⁺ doped silicon thin film and waveguides for mid-infrared sources," *Applied Physics Letters*, 101, 141107 (2012).
- [74] Choi, H. K., Editor, [Longwavelength Infrared Semiconductor Lasers] John Wiley & Sons (2004) ISBN 0-471-39200-6
- [75] Lee, C. S., Frost, T., Guo, W. and Bhattacharya, P., "Integration of 1.3- μm quantum-dot lasers with Si₃N₄ waveguides for single mode optical interconnects," *IEEE Journal of Quantum Electronics* 48, 1346-1351 (2012).
- [76] Lin, H., Zou, Y. Danto, S., Musgraves, J. D., Richardson, K., Lin, P.T., Vivek, S., Agarwal, A., Kimerling, L.C. and Hu, J., "Mid-infrared As₂Se₃ chalcogenide glass-on-silicon waveguides," Digest, IEEE 9th Intl. Conf. on Group IV Photonics, 246-248 San Diego (29 Aug 2012).
- [77] Soref, R. A., Menendez J. and Kouvetakis, J., "Epitaxial Ge, GeSn and SiGeSn materials for new optoelectronic applications," invited paper, 4th International SiGe Devices and Technology Meeting, Hsinchu, Taiwan (11 May 2008).
- [78] Moontragoon, P., Soref, R. A. and Ikonik, Z., "The direct and indirect bandgaps of unstrained SixGe1-x-ySny and their photonic device applications," *Journal of Applied Physics* 112, 073106 (2012).
- [79] Sun, G., and Soref, R. A., "Design of a Si-based lattice-matched room-temperature SiGeSn/GeSn/SiGeSn multi-quantum-well mid-infrared laser diode," *Optics Express* 19, 19957-19965 (2010).
- [80] Sun, G., Soref, R. A. and Cheng, H. H., "Design of an electrically pumped SiGeSn/GeSn/SiGeSn double-heterostructure mid-infrared laser," *Journal of Applied Physics* 108(3), 033107 (2010).

- [81] Cheng, H. H., Sun, G. and Soref, R., "Mid-infrared electroluminescence from a Ge/Ge_{0.96}Sn_{0.04}/Ge double heterostructure p-i-n diode on a Si substrate," submitted to Applied Physics Letters (2013).
- [82] Kasper, E., "GeSn light-emitting pin diodes on Si," IEEE 9th Intl. Conf. on Group IV Photonics, San Diego, Digest 311-313 (2012).
- [83] Gassanq, A., Gencarelli, F., Van Campenhout, J., Shimura, Y., Loo, R., Narcy, G., Vincent, B. and Roelkens, G., "GeSn/Ge heterostructure short-wave infrared photodetectors on silicon," Optics Express 20, 27297-27303 (2012).
- [84] Nedeljkovic, M., Soref, R. A. and Mashanovich, G. Z., "Free-carrier electrorefraction and electroabsorption modulation predictions for silicon over the 1-14 μm infrared wavelength range," IEEE Photonics Journal 3(6), 1171-1180 (2011).
- [85] Nedeljkovic, M., Soref, R. A. and Mashanovich, G. Z., "Free-carrier electro-absorption and electro-refraction modulation in group IV materials at mid-infrared wavelengths," SPIE Photonics West, paper 8266-31, San Jose, CA (25 Jan 2012).
- [86] Van Camp, M. A., Asseta, S., Gill, D. M., Barwicz, T., Shank, S. M., Rice, P. M., Topuria, T. and Green, W. M. J., "Demonstration of electrooptic modulation at 2165 nm using a silicon Mach-Zehnder interferometer," Optics Express 20, 28009-28016 (2012).
- [87] Soref, R., Sun, G. and Cheng, H. H., "Franz-Keldysh electro-absorption modulation in germanium-tin alloys," Journal of Applied Physics 111, 123113 (2012).
- [88] Zhang, L., Lin, Q., Yue, Y., Yan, Y., Beausoleil, R. G., Agarwal, A., Kimerling, L. C., Michel, J. and Wilner, A. E., "On-chip octave-spanning supercontinuum in nanostructured silicon waveguides using ultralow pulse energy," IEEE Journal of Selected Topics in Quantum Electronics 18(6), 1799-18?? (2012).
- [89] Hon, N. K., Soref, R. A. and Jalali, B., "The third-order nonlinear optical coefficients of Si, Ge, and Si_{1-x}Ge_x in the midwave and longwave infrared," Journal of Applied Physics 110, 011301 (2011).
- [90] Jalali, B., Soref, R., Hon, N. K. and Borlaug, D., "Silicon photonics in midwave and longwave infrared", (invited) 11th Intl. Conf. on Mid-infrared Optoelectronics, Materials and Devices (MIOMD-XI), Evanston, IL (4 Sept. 2012).
- [91] Avrutsky, I. and Soref, R., "Phase-matched sum frequency generation in strained silicon waveguides using their second-order nonlinear optical susceptibility," Optics Express 19, 21707-21716 (2011).
- [92] Avrutsky, I., Soref, R. and Buchwald, W. "Phase matching and threshold condition in a guided-wave optical parametric oscillator," Digest of Nonlinear Optics Conference (NLO) Optical Society of America, Kauai, Hawaii (17-22 July 2011).
- [93] Liu, X., Kuyken, B., Roelkens, G., Baets, R., Osgood, R. M. and Green, W. M. J., "Bridging the mid-infrared-to-telecom gap with silicon nanophotonic spectral translation," Nature Photonics 6, 667-671 (2012). *Supplementary Information online*, DOI:10.1038/NPhoton.2012.221, 12 Sept 2012.
- [94] Wang, Z., Liu, H., Huang, N., Sun, Q. and Wen, J., "Efficient terahertz-wave generation via four-wave mixing in silicon membrane waveguides," Optics Express 20(8), 8920-8928 (2012).

Light in a Twist: Optical Angular Momentum

Miles J. Padgett

School of Physics and Astronomy, University of Glasgow, Scotland UK,

ABSTRACT

In 1992 Allen et al. recognized that light beams could carry an angular momentum in addition to that arising from the photon spin. This orbital angular momentum can be created using lenses or diffractive optics, the later often formed using liquid crystal displays. Both whole beams and single photons can carry this twist, and transfer it to particles causing them to spin. This paper introduces the underlying principles of orbital angular momentum and reviews a number of its manifestations and applications. These effects highlight how optics still contains surprises and opportunities for manipulation, imaging and communication in both the classical and quantum worlds.

Keywords: Optical Angular Momentum

1. INTRODUCTION

The linear momentum of light was known, or at least postulated, since the time of Kepler who suggested that the resulting optical radiation pressure was the reason why comet tails always pointed away from the sun. More formally, the linear momentum of light, a prediction from Maxwell's equations [1], was shown in 1901 by Lebedew [2] to induce the recoil and rotation of a suspended mechanical object. The angular momentum of a light beam is also derivable from Maxwell's equations but was explicitly considered by Poynting who drew analogies between optical and mechanical systems to suggest that for a beam of circularly polarized light, the ratio between its angular momentum and its energy was $1/\omega$ [3], where ω is the angular frequency of the light. Poynting himself thought that the torque exerted by a light beam on any object would be too small to observe, however, in 1936 Beth succeeded in doing just this [4]. He showed that a birefringent waveplate, suspended by a fine thread, experienced a torque in reaction to a change in the polarization state of the transmitted light. This early work made no reference to quantization or photons, rather addressed the problem in terms of energy to momentum ratios. Nowadays accepting the concept of a photon with an energy $\hbar\omega$ leads directly to the familiar descriptions of the linear and spin angular momentum of the photon being $\hbar k$ and \hbar respectively, where $k = 2\pi/\lambda$.

The \hbar quantization of the spin angular momentum of the photon is completely consistent with a photon interpretation of the interaction of light and electronic dipole transitions within atomic systems. Beyond dipole transitions, where the angular momentum exchange is \hbar , in 1932 Darwin (grandson of the originator of evolution) recognized that higher-order transitions required an optical angular momentum corresponding to integer multiples of \hbar [5]. He postulated that this extra momentum could be generated as a recoil torque arising if the center of mass of the atomic system was slightly displaced from the optical emission axis.

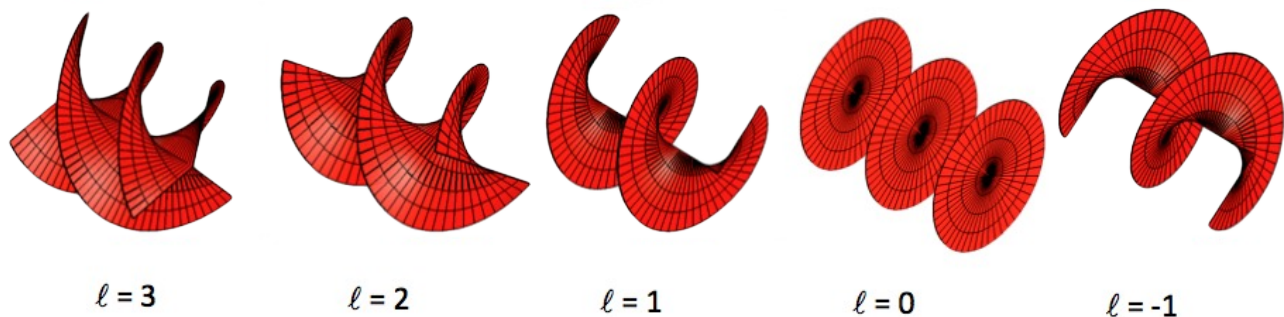


Figure 1. The helical phase fronts corresponding to various values of OAM

Despite this appreciation of non-spin angular momentum within optical fields it was not until 1992 that Allen, Woerdman and co-workers recognized that a beam with helical phase fronts described by a phase cross-section of $\exp(i\ell\theta)$, see figure 1, has an angular momentum to energy ratio of ℓ/ω , hence an angular momentum per photon of $\ell\hbar$ [6]. This orbital angular momentum is distinct from, and additional to, the spin angular momentum associated with the polarization state of the light.

The helical nature of the phase fronts means that the Poynting vector associated with helically-phased beams is not collinear with the propagation direction. A simple geometrical construction shows the $\exp(i\ell\theta)$ phase term implies at each position within the beam that the local Poynting vector is angled with respect to the beam axis by an angle given by $\beta = \ell/kr$, where r is the radius from the beam axis [7]. Within a ray optical picture, this angle describes the skew angle of the rays [8] and if each ray is considered to represent a photon with linear momentum $\hbar k$ then this simply corresponds to an angular momentum along the beam axis of $L = \hbar k \times r \times \ell/kr = \ell\hbar$ [9], compatible with more rigorous treatments [10]. This circulation of optical energy and momentum around the beam axis leads to helical phase fronts also being called optical vortices [11].

2. GENERATING BEAMS CONTAINING ORBITAL ANGULAR MOMENTUM

Although the 1992 recognition of the orbital angular momentum (OAM) of light was in the context of helically-phased beam, the beams themselves had been studied for a number of years. Closely related to the existence of helical phase fronts are the concepts of phase singularities and optical vortices. The $\exp(i\ell\theta)$ phase structure, by definition, implies a position at the exact center of the beam where the phase is not defined; a phase-singularity. Rather than being an esoteric property of exotic beams, phase singularities are a natural consequence of random wave fields. For example, the familiar optical speckle pattern created whenever an extended laser beam is scattered from a rough surface contains numerous black points. Each of these points is a position of zero intensity immediately around which the phase is described by $\exp(i\ell\theta)$, where $\ell = \pm 1$. But the location of these phase singularities is not restricted to one plane, the interfering waves extend over all space and these points of darkness within a plane are simply a section through lines of darkness that percolate all of space [12].

Rather than using optical speckle, initial studies into singularities within random fields were performed by Nye and Berry with acoustics, using ultrasonic beams reflected from rough surfaces [13]. Their original motivation behind this work was to better understand radio wave echoes from ice sheets, the main observation being that the reflected field contained intensity nulls around which the phase changed by 2π . Subsequent work examined optical systems, again showing that the fields naturally contained phase singularities [14].

The potential for gas discharge lasers to produce optical beams containing a single phase singularity along the beam axis was recognized and analyzed by Vaughan and Willets [15]. Subsequent work by Tamm and Weiss showed that precise control of the degeneracy of the Hermite-Gaussian modes, again within a gas discharge laser, could form a stable helically-phased superposition [16,17].

In 1990 Soskin and co-workers developed the use of diffraction gratings containing a fork dislocation to generate a helically phased beam in the first diffracted order [18], independently similar work was also reported Heckenberg et al. [19], see figure 2. These forked diffraction gratings are now the most common method for both the generation and detection of beams carrying OAM but at the time of their initial demonstration the implications for angular momentum had not been recognized. The use of diffractive optics for the generation of helical-phased and other exotic beams types has been revolutionized by the commercial availability of spatial light modulators that are pixelated liquid crystal, display-type, devices that introduce a spatially programmable phase change in the reflected light. This flexibility was applied to the generation of multiple beam types within optical tweezers [20] but is now ubiquitous throughout the study and application of complex light fields [21].

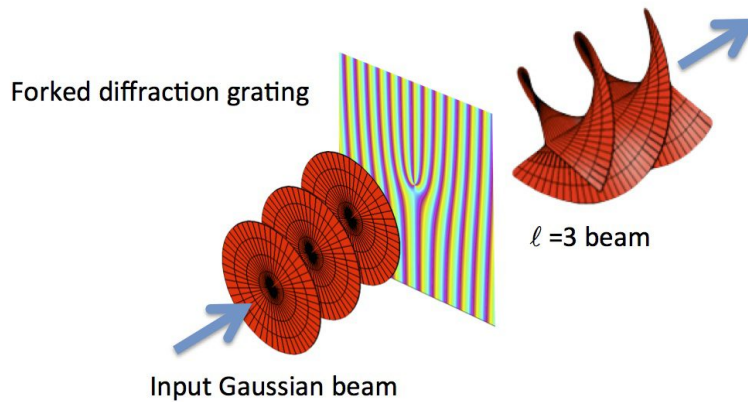


Figure 2. A forked diffraction grating can transform a Gaussian beam to a beam with helical phase front. In this case the grating is a blazed phase grating to maximize the diffraction into the first-order beam.

3. APPLICATION OF OAM TO MICROMANIPULATION

Immediately following the 1992 recognition of OAM within light beams that could be generated within the laboratory, effort was devoted to the demonstration of the transfer of this angular momentum to macroscopic objects. However, this goal is extremely challenging since if the axis of the beam is not accurately aligned with the rotation axis of the suspended object then the linear momentum of the light beam will exert a torque on the object which may be many times higher than that exerted by the OAM alone. This problem was overcome by Rubinsztein-Dunlop and co-workers who performed an experiment in optical tweezers where an $\ell = 3$ beam was used to both trap an absorbing microscopic particle and set into rotation by an angular momentum transfer [22]. In this experiment the use of the same beam to set the rotation axis and provide the torque removed any issues with the alignment of a mechanical constraint, removing the potential torque created by the linear momentum acting about a radius vector. Later work extended these studies to consider the simultaneous transfer of both spin and orbital angular momentum where their relative handedness could give addition or subtraction to speed up or slow down the particle rotation [23,24]. For larger beams, the different behavior of spin and orbital angular momentum could also be observed [25]. Whereas the transfer of spin angular momentum causes particles to spin around their own axis, the transfer of OAM causes them to orbital around the beam axis, confined at the radius corresponding to the highest intensity of the beam, see figure 3. These demonstrations of “optical spanners” did much to promote interest in both orbital angular momentum and optical tweezers, the instant appeal being that of creating optically driven micromachines and studies of colloidal systems [20,26].

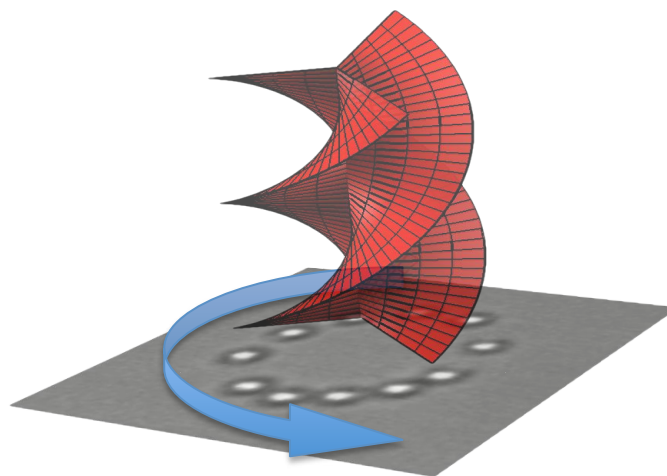


Figure 3. A solution of micron-sized colloids suspended in water. When illuminated by helically-phased light the particles are set in rotation

4. PHENOMENOLOGY OF OAM IN LIGHT

At the most fundamental level, the Laguerre-Gaussian laser modes that conveniently describe orbital angular momentum states are just one complete basis set from which all optical beams can be synthesized. Many other modal sets exist, not least the Hermite-Gaussian family of laser modes, and all the sets of modes could be applied to reach identical solutions to a variety of problems. However, just as with polarization, where problems lends themselves to solving in either the linear or circular basis, the description of a problem in terms of OAM can sometimes lead to an intuitive understanding not apparent within other basis sets.

Problems that lend themselves to a treatment in terms of OAM states are those involving circular symmetry and/or rotation about a given axis. The linear Doppler shift is a well-known phenomenon where the relative velocity, v , between the light source and the observer gives a frequency shift of $\Delta f = f_0 v/c$, where f_0 is the unshifted frequency and c is the speed of light. Much less well-known is the rotational or angular Doppler effect [27,28]. For rotational motion of angular frequency Ω between source and observer, the frequency shift is $\Delta f = (\ell + \sigma)\Omega/2\pi$, where $\sigma = \pm 1$ for right- and left-handed circularly polarized light, and $j = \ell + \sigma$ is the total angular momentum per photon [29]. Although an intuitive result, the mechanism by which the polarization (spin) and the helical phase structure (orbital) can combine is intriguing. Plotting the cross-section through the beam circularly polarized, helically-phase beam reveals a vector field pattern that is $\ell + \sigma$ fold rotationally symmetric, hence rotating the beam once, advances/retards the phase by $\ell + \sigma$ cycles.

The Heisenberg uncertainty principle arises from wave-particle duality and is a natural consequence of Fourier-theory. It relates the standard deviation Δx of the position distribution by a Fourier-transform to the standard deviation Δp_x of the momentum distribution, $\Delta x \Delta p_x \geq \hbar/2$. A reasonable question to ask is what is the angular equivalent? Unlike the linear position, which is both continuous and unbounded, the angular variable although continuous is restricted to be periodic within a $\pm\pi$ range. The periodic nature of the angular variable means that the relationship to angular momentum is via a Fourier-series, leading to a natural quantization of the momentum. For restricted angular distributions the standard deviations of position and angular momentum is given by $\Delta\theta\Delta\ell\hbar \geq \hbar/2$. In the other extreme of an unbounded angle, the angular standard deviation remains finite and hence this simple form of the angular uncertainty relationship needs to be modified. Several approaches have been taken to this problem [30] but, for angular distributions centered at $\theta = 0$, the one closest in formulation to the linear case is given as $\Delta\theta\Delta\ell\hbar \geq (1 - 2\pi P_{\theta=\pm\pi})\hbar/2$, where $P_{\theta=\pm\pi}$ is the probability density of the position distribution at $\theta = \pm\pi$ [31]. In both these examples of rotational Doppler and uncertainty relationships, a description in terms of an OAM index ℓ gives simple formulae clearly analogous to the better known linear examples.

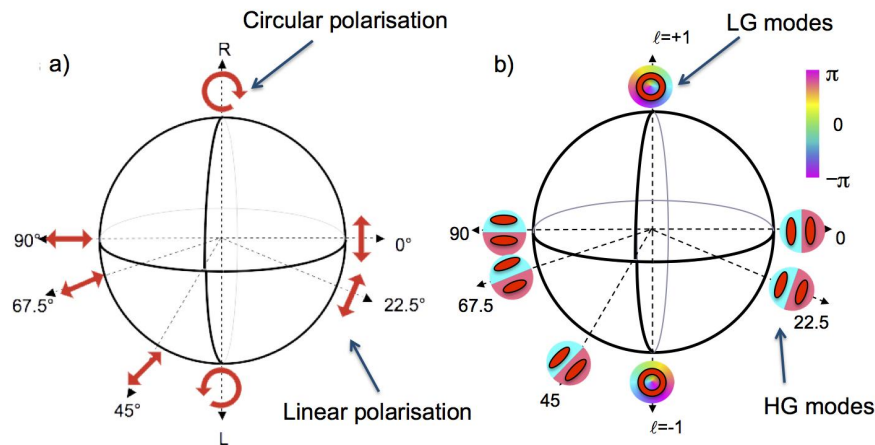


Figure 4. a) A Poincaré sphere representation of polarization and the Poincaré sphere equivalent for Laguerre-Gaussian and Hermite Gaussian first-order modes

In the original work of Allen, Woerdman and co-workers their generation of OAM beams was based on a transformation between Hermite-Gaussian and Laguerre-Gaussian laser modes [32]. They showed that by ingenious use of cylindrical

lenses they could use the mode dependent Gouy phase to take any Hermite Gaussian mode with indices m and n and transform it into a helically-phased Laguerre-Gaussian mode with indices $\ell = m - n$ and $p = \min(m, n)$, where ℓ has its usual meaning and p describes the number of radial rings in the mode. This introduction of a phase shift between Hermite-Gaussian modes by the cylindrical lenses is completely analogous to the shift introduced between linear polarization states by a birefringent waveplate. This mathematical analogy between descriptions of orbital and spin angular momentum states extends to optical activity, where the resulting rotation in polarization states is analogous in orbital angular momentum to the rotation of an image [33]. The analogy can usefully be illustrated and, as we shall see later, applied in terms on an orbital angular momentum equivalent to the Poincaré sphere [34], see figure 4, and /or equivalent Jones Matrices [35].

5. APPLICATION OF OAM IN QUANTUM OPTICS

As discussed in the introduction, OAM plays an important role in high-order atomic transitions and hence we should not be surprised that OAM is not just an ensemble property of many photons, but applies to single photons too. Shortly after the initial investigations into OAM optical manipulation, studies were also reported relating to the use of OAM within nonlinear optics. In a simple photon interpretation, the process of frequency doubling takes place within a nonlinear crystal where two incident photons of frequency ω combine to give a single emitted photon of frequency 2ω in a process which conserves both the optical energy and linear momentum of the light. Given that OAM is derived from the azimuthal component of the momentum it is reasonable, and it transpires correct, to assume that the OAM is conserved too. This conservation leads to two incident photons with frequency ω and OAM of $\ell\hbar$ combining to give an output photon of 2ω and OAM of $2\ell\hbar$ [36], see figure 5. The inverse of frequency doubling is parametric down-conversion where a single incident pump photon produces two output signal and idler photons of lower frequency. Within this process the conservation of both energy and momentum means that this method is widely used in the preparation of entangled photon pairs for studies in quantum optics. In 2001 Zeilinger and co-workers demonstrated that the conservation of OAM meant the emitted photons were entangled in their OAM. Previously it had been shown that for a pump beam with $\ell = 0$, the down-converted photons have a wide range of ℓ values [37], but Zeilinger's work showed that although the range was large, the OAM of every photon pair was always such that $\ell_{signal} = -\ell_{idler}$ [38]. This work required the measurement of the OAM of single photons. Whereas forked diffraction gratings had previously been used to convert the output of a single mode optical fiber into a helically-phased beam, Zeilinger and co-workers reversed the process to selectively couple helically-phased photons back into the fiber. By physically interchanging the diffraction gratings with different number of forks in the signal and idler arms of the experiment it was possible to measure the correlation between the signal and idler photons over a range of ℓ values. Beyond entanglement itself it was suggested, and shown, that this entanglement has applications in multibit communication protocols [39-41].

In a similar fashion as had been shown previously for optical manipulation [20], the versatility of these OAM entanglement experiments were later transformed by replacement of the static diffraction gratings by SLMs, which could simply be reprogrammed to test for different states [42]. The use of SLMs for measuring the entanglement of spatial states has been widespread allowing OAM based demonstrations of EPR [43], violations of Bell inequalities at low [44] and at very high quantum number [45], and entanglement of both OAM and radial modes [46]. In many of these cases, the formulation of entanglement test relied heavily upon the analogies that can be drawn between polarization and helical phase through state representation on the Poincaré sphere.

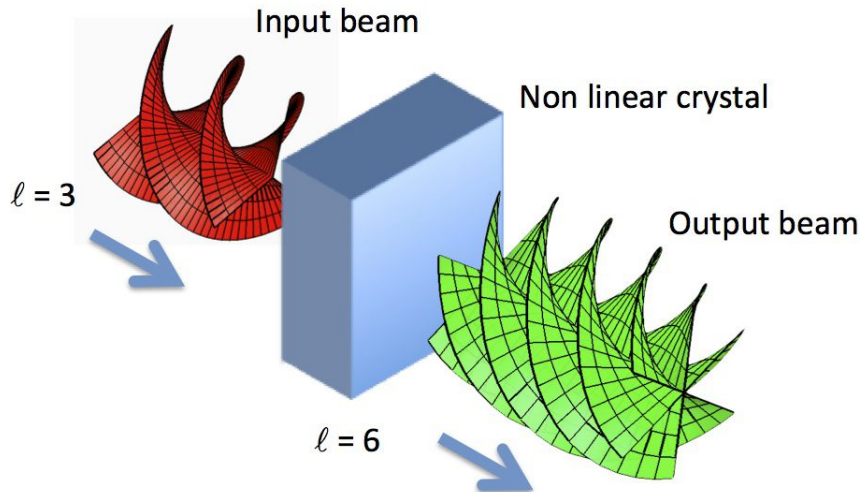


Figure 5. Second harmonic generation by a non linear crystal doubles both the energy and OAM of each photon. Note that this mutual doubling maintains the skew angle of the phase fronts.

6. APPLICATION OF OAM IN COMMUNICATION SYSTEMS

Compared to the two dimensional state-space of polarization, the unbounded state-space of OAM immediately suggests its use as a variable in data communication and processing. This opportunity applies not just to quantum systems but in the classical regime too. An early demonstration of using OAM within a simple communication system was in 2004 where SLMs were used to both generate and measure the OAM in a laser beam between a send and a receive telescope [47]. Since that time, a number of demonstrations have been made of OAM as a route to spatial channel multiplexing. OAM is not just an optical property but applies to all wave-fields where the spatial phase distribution can be spatially controlled. Within the electromagnetic spectrum, OAM has been discussed in X-ray [48], microwave [49] and radio-wave [50] frequencies. For radio-waves this demonstration involved the co-axial propagation and detection of $\ell = 0$ and $\ell = 1$ beams, each modulated to transmitted an independent audio channel. In the optical regime multiple OAM channels have been created using SLMs to give spatial mode multiplexing to demonstrate >Terabit communication rates [51]. For application in quantum cryptography, where the larger number of states gives both more information and higher security, an SLM system has been shown where the two unbiased basis sets used were orbital angular momentum and angular position [52].

For all communication systems based on OAM the technical challenge is the efficient measurement of the OAM state. Measurement of the polarization state and hence the SAM of a light beam is readily accomplished using a polarizing beam splitter. OAM is more problematic. For many photons in the same state, the interference of beam with a plane wave gives an interference pattern comprising a straight-line fringe pattern with ℓ dislocations. Other interference effects include the analysis of the patterns produced by double slits [53] or more complicated apertures [54] [55]. However, all interference techniques require many photons to form a complete pattern and therefore, although appropriate for classical beams, clearly they cannot form the basis of measuring the OAM of a single photon.

As discussed the first single photon measurement of the OAM used a diffractive optical element, similar to those used for the generation [38]. An incoming beam with an $\exp(i\ell\theta)$ phase dependence is diffracted to give a Gaussian beam that can be coupled into the single mode fiber connected to a single photon detector (all other values of ℓ result in no coupling into the fiber). However, every photon can only be tested for one particular value of ℓ . More sophisticated diffractive optical elements can be designed that are capable of detecting several OAM state simultaneously but only with an inherent efficiency that does not exceed the reciprocal of the number of states to be tested.

Recently reported was a new measurement technique for the OAM of an input beam such that every OAM state is focused to a different lateral position at the output [56]. This approach was inspired by the ease at which plane-waves

propagating in different directions can be distinguished from each other. If focused by a lens, each plane-wave direction gives a bright spot in the focal plane of the lens with a transverse position related to the angular direction of the incoming wave. If the direction change corresponds to an additional phase change of 2π across the aperture of the lens then the separation of the spots is comparable to that of the Rayleigh resolution criterion. For measuring OAM, two optical components transform every helically-phased input beam of the form $\exp(i\ell\theta)$ to a plane-wave output with a transverse phase change of $2\pi\ell$. A final lens brings this plane-wave to a focus at a lateral position dependent upon the transverse phase change and hence dependent on the input OAM value [57].

7. APPLICATION OF OAM IN IMAGING SYSTEMS

Optical polarization, hence spin angular momentum, plays a useful role in microscopy and orbital angular momentum does too. In 2001 Swartzlander proposed that introducing a OAM mask (equivalent to a forked diffraction grating) into a telescope was a form of spatial filtering which could suppress a spatially coherent or point light source from an image, revealing other low intensity features [58]. Since that time, this concept has been further developed within a proposal to use it to suppress light from the astronomical observation of a bright star so the neighboring planets are easier to spot [59].

At the other size extreme, OAM has also proved an interesting parameter within microscopy [60] and imaging [61]. Phase filters are commonly used within microscopy to enhance the image contrast of nearly transparent objects. Ritsch-Marte and co-workers showed that forked diffraction grating placed into the image train gives unidirectional edge enhancement of phase objects [62]. This enhancement arises since a phase step corresponds to a superposition of right and left OAM states, imaging either one of these states highlights the edges in the object. Extending the use of OAM beams as reference beams within an interferometer gives interferograms where the fringes become spirals, the sense of which denotes whether the surface feature is a hill or a depression [63].

8. CONCLUDING COMMENTS

From a classical perspective, OAM is fully described by 19th century electromagnetism and similarly in the quantum regime it is simply one example of a spatial state. The Laguerre-Gaussian modes with which OAM is often described are a complete orthonormal set and as such can be described in terms of superpositions of other well known modes, such as Hermite-Gaussian or indeed plane waves. However, over the course of the last 21 years, studies of OAM have attracted significant interest in the use of these and other non-traditional spatial modes in applications ranging from optical manipulation to imaging. Beyond applications, the analysis of problems in this angular basis has provided new insight to problems ranging from rotational frequency shifts to angular uncertainty. In quantum science, OAM emphasized spatial modes as one parameter within a large state space thereby giving a convenient basis set for new tests and demonstrations of high-dimensional entanglement. Most generally, OAM has reminded us that when considering the optical behavior of a light beam, intensity alone is not enough, rather the phase-structure of the beam is of equal, if not more, importance. Hopefully OAM will continue to inform and contribute to modern optics over the next 21 years too.

REFERENCES

- [1] J. C. Maxwell, "A dynamical theory of the electromagnetic field," *Philosophical Transactions for the Royal Society of London*. (1865).
- [2] P. Lebedew, "Untersuchungen über die Druckkräfte des Lichtes," *Annalen der Physik* **311**(11), 433–458, Wiley Online Library (1901).
- [3] J. H. Poynting, "The wave motion of a revolving shaft, and a suggestion as to the angular momentum in a beam of circularly polarised light," *Proc R Soc Lon Ser-A* **82**, 560–567 (1909).
- [4] R. A. Beth, "Mechanical detection and measurement of the angular momentum of light," *Physical Review* **50**(2), 115–125 (1936).
- [5] C. G. Darwin, "Notes on the Theory of Radiation," *Proc R Soc Lon Ser-A* **136**(829), 36–52 (1932).
- [6] L. Allen, M. W. Beijersbergen, R. J. C. Spreeuw, and J. P. Woerdman, "Orbital angular-momentum of light and the transformation of Laguerre-Gaussian laser modes," *Phys Rev A* **45**(11), 8185–8189 (1992).
- [7] M. J. Padgett and L. Allen, "The Poynting vector in Laguerre-Gaussian laser modes," *Opt Commun* **121**(1-3),

36–40 (1995).

- [8] J. Courtial and M. J. Padgett, “Limit to the orbital angular momentum per unit energy in a light beam that can be focussed onto a small particle,” *Opt Commun* **173**(1-6), 269–274 (2000).
- [9] V. Garces-Chavez, D. McGloin, M. Padgett, W. Dultz, H. Schmitzer, and K. Dholakia, “Observation of the Transfer of the Local Angular Momentum Density of a Multiringed Light Beam to an Optically Trapped Particle,” *Phys Rev Lett* **91**(9), 093602 (2003).
- [10] L. Allen, M. J. Padgett, and M. Babiker, “The orbital angular momentum of light,” *Prog Optics* **39**, 291–372 (1999).
- [11] P. Couillet, G. Gil, and F. Rocca, “Optical vortices,” *Opt Commun* **73**(5), 403–408 (1989).
- [12] K. O’Holleran, M. R. Dennis, F. Flossmann, and M. J. Padgett, “Fractality of light’s darkness,” *Phys Rev Lett* **100**(5), 053902 (2008).
- [13] J. F. Nye and M. V. Berry, “Dislocations in wave trains,” *Proc R Soc Lon Ser-A* **336**(1605), 165–190 (1974).
- [14] M. V. Berry, J. F. Nye, and F. Wright, “The Elliptic Umbilic Diffraction Catastrophe,” *Philosophical Transactions for the Royal Society of London*. **291**, 453–484 (1979).
- [15] J. M. Vaughan and D. C. Willetts, “Interference properties of a light-beam having a helical wave surface,” *Opt Commun* **30**(3), 263–267 (1979).
- [16] C. Tamm, “Frequency locking of 2 transverse optical modes of a laser,” *Phys Rev A* **38**(11), 5960–5963 (1988).
- [17] C. Tamm and C. O. Weiss, “Bistability and optical switching of spatial patterns in a laser,” *J Opt Soc Am B* **7**(6), 1034–1038 (1990).
- [18] V. Y. Bazhenov, M. V. Vasnetsov, and M. S. Soskin, “Laser-beams with screw dislocations in their wave-fronts,” *Jetp Lett* **52**(8), 429–431 (1990).
- [19] N. R. Heckenberg, R. McDuff, C. P. Smith, and A. G. White, “Generation of optical phase singularities by computer-generated holograms,” *Opt Lett* **17**(3), 221–223 (1992).
- [20] D. G. Grier, “A revolution in optical manipulation,” *Nature* **424**, 810–816 (2003).
- [21] A. M. Yao and M. J. Padgett, “Orbital angular momentum: origins, behavior and applications,” *Adv. Opt. Photon.* **3**(2), 161 (2011).
- [22] H. He, M. E. J. Friese, N. R. Heckenberg, and H. Rubinsztein-Dunlop, “Direct observation of transfer of angular momentum to absorptive particles from a laser beam with a phase singularity,” *Phys Rev Lett* **75**(5), 826–829 (1995).
- [23] M. E. J. Friese, J. Enger, H. Rubinsztein-Dunlop, and N. R. Heckenberg, “Optical angular-momentum transfer to trapped absorbing particles,” *Phys Rev A* **54**(2), 1593–1596 (1996).
- [24] N. B. Simpson, K. Dholakia, L. Allen, and M. J. Padgett, “Mechanical equivalence of spin and orbital angular momentum of light: an optical spanner,” *Opt Lett* **22**(1), 52–54 (1997).
- [25] A. T. O’Neil, I. MacVicar, L. Allen, and M. J. Padgett, “Intrinsic and extrinsic nature of the orbital angular momentum of a light beam,” *Phys Rev Lett* **88**(5), 053601 (2002).
- [26] M. Padgett and R. Bowman, “Tweezers with a twist,” *Nat Photonics* **5**, 343–348 (2011).
- [27] B. A. Garetz, “Angular Doppler Effect,” *J Opt Soc Am* **71**(5), 609–611 (1981).
- [28] I. Bialynicki-Birula and Z. Bialynicka-Birula, “Rotational frequency shift,” *Phys Rev Lett* **78**, 2539–2542 (1997).
- [29] J. Courtial, D. A. Robertson, K. Dholakia, L. Allen, and M. J. Padgett, “Rotational frequency shift of a light beam,” *Phys Rev Lett* **81**(22), 4828–4830 (1998).
- [30] G. W. Forbes, M. A. Alonso, and A. E. Siegman, “Uncertainty relations and minimum uncertainty states for the discrete Fourier transform and the Fourier series,” *J. Phys. A: Math. Gen* **36**(25), 7027–7047 (2003).
- [31] S. Franke-Arnold, S. M. Barnett, E. Yao, J. Leach, J. Courtial, and M. Padgett, “Uncertainty principle for angular position and angular momentum,” *New J Phys* **6**, 103 (2004).
- [32] M. W. Beijersbergen, L. Allen, H. E. L. O. van der Veen, and J. P. Woerdman, “Astigmatic laser mode converters and transfer of orbital angular momentum,” *Opt Commun* **96**(1-3), 123–132 (1993).
- [33] L. Allen and M. Padgett, “Equivalent geometric transformations for spin and orbital angular momentum of light,” *J Mod Optic* **54**(4), 487–491 (2007).
- [34] M. J. Padgett and J. Courtial, “Poincare-sphere equivalent for light beams containing orbital angular momentum,” *Opt Lett* **24**(7), 430–432 (1999).
- [35] L. Allen, J. Courtial, and M. J. Padgett, “Matrix formulation for the propagation of light beams with orbital and spin angular momenta,” *Phys Rev E* **60**(6), 7497–7503 (1999).

- [36] K. Dholakia, N. B. Simpson, M. J. Padgett, and L. Allen, "Second-harmonic generation and the orbital angular momentum of light," *Phys Rev A* **54**(5), R3742–R3745 (1996).
- [37] J. Arlt, K. Dholakia, L. Allen, and M. J. Padgett, "Parametric down-conversion for light beams possessing orbital angular momentum," *Phys Rev A* **59**(5), 3950–3952 (1999).
- [38] A. Mair, A. Vaziri, G. Weihs, and A. Zeilinger, "Entanglement of the orbital angular momentum states of photons," *Nature* **412**(6844), 313–316 (2001).
- [39] A. Vaziri, G. Weihs, and A. Zeilinger, "Experimental Two-Photon, Three-Dimensional Entanglement for Quantum Communication," *Phys Rev Lett* **89**(24), 240401 (2002).
- [40] N. K. Langford, R. Dalton, M. Harvey, J. L. O'Brien, G. J. Pryde, A. Gilchrist, S. D. Bartlett, and A. G. White, "Measuring entangled qutrits and their use for quantum bit commitment," *Phys Rev Lett* **93**(5), 053601 (2004).
- [41] G. Molina-Terriza, J. P. Torres, and L. Torner, "Twisted photons," *Nat Phys* **3**(5), 305–310 (2007).
- [42] E. Yao, S. Franke-Arnold, J. Courtial, M. J. Padgett, and S. M. Barnett, "Observation of quantum entanglement using spatial light modulators," *Opt Express* **14**(26), 13089–13094 (2006).
- [43] J. Leach, B. Jack, J. Romero, A. K. Jha, A. M. Yao, S. Franke-Arnold, D. G. Ireland, R. W. Boyd, S. M. Barnett, et al., "Quantum Correlations in Optical Angle-Orbital Angular Momentum Variables," *Science* **329**(5992), 662–665 (2010).
- [44] J. Leach, B. Jack, J. Romero, M. Ritsch-Marte, R. W. Boyd, A. K. Jha, S. M. Barnett, S. Franke-Arnold, and M. J. Padgett, "Violation of a Bell inequality in two-dimensional orbital angular momentum state-spaces," *Opt Express* **17**(10), 8287–8293 (2009).
- [45] R. Fickler, R. Lapkiewicz, W. N. Plick, M. Krenn, C. Schaeff, S. Ramelow, and A. Zeilinger, "Quantum Entanglement of High Angular Momenta," *Science* **338**, 640–643 (2012).
- [46] V. D. Salakhutdinov, E. R. Eliel, and W. Löffler, "Full-Field Quantum Correlations of Spatially Entangled Photons," *Phys Rev Lett* **108**, 173604 (2012).
- [47] G. Gibson, J. Courtial, M. J. Padgett, M. Vasnetsov, V. Pas'ko, S. M. Barnett, and S. Franke-Arnold, "Free-space information transfer using light beams carrying orbital angular momentum," *Opt Express* **12**(22), 5448–5456 (2004).
- [48] S. Sasaki and I. McNulty, "Proposal for Generating Brilliant X-Ray Beams Carrying Orbital Angular Momentum," *Phys Rev Lett* **100**(12), 124801 (2008).
- [49] G. A. Turnbull, D. A. Roberson, G. M. Smith, L. Allen, and M. J. Padgett, "Generation of free-space Laguerre-Gaussian modes at millimetre-wave frequencies by use of a spiral phaseplate," *Opt Commun* **127**(4-6), 183–188 (1996).
- [50] F. Tamburini, E. Mari, A. Sponselli, B. Thidé, A. Bianchini, and F. Romanato, "Encoding many channels on the same frequency through radio vorticity: first experimental test," *New J Phys* **14**(3), 033001 (2012).
- [51] J. Wang, J.-Y. Yang, I. M. Fazal, N. Ahmed, Y. Yan, H. Huang, Y. Ren, Y. Yue, S. Dolinar, et al., "Terabit free-space data transmission employing orbital angular momentum multiplexing," *Nat Photonics* **6**(7), 488–496, Nature Publishing Group (2012).
- [52] M. Malik, M. O'Sullivan, B. Rodenburg, M. Mirhosseini, J. Leach, M. P. J. Lavery, M. J. Padgett, and R. W. Boyd, "Influence of atmospheric turbulence on optical communications using orbital angular momentum for encoding," *Opt Express* **20**(12), 13195–13200 (2012).
- [53] H. I. Sztul and R. R. Alfano, "Double-slit interference with Laguerre-Gaussian beams," *Opt Lett* **31**(7), 999–1001 (2006).
- [54] G. C. G. Berkhout and M. W. Beijersbergen, "Method for Probing the Orbital Angular Momentum of Optical Vortices in Electromagnetic Waves from Astronomical Objects," *Phys Rev Lett* **101**(10), 100801 (2008).
- [55] J. M. Hickmann, E. J. S. Fonseca, W. C. Soares, and S. Chávez-Cerda, "Unveiling a Truncated Optical Lattice Associated with a Triangular Aperture Using Light's Orbital Angular Momentum," *Phys Rev Lett* **105**, 053904 (2010).
- [56] G. C. G. Berkhout, M. P. J. Lavery, J. Courtial, M. W. Beijersbergen, and M. Padgett, "Efficient Sorting of Orbital Angular Momentum States of Light," *Phys Rev Lett* **105**(15), 153601 (2010).
- [57] M. P. J. Lavery, D. J. Robertson, G. C. G. Berkhout, G. D. Love, M. J. Padgett, and J. Courtial, "Refractive elements for the measurement of the orbital angular momentum of a single photon," *Opt Express* **20**(3), 2110–2115 (2012).
- [58] G. A. Swartzlander, "Peering into darkness with a vortex spatial filter," *Opt Lett* **26**(8), 497–499 (2001).
- [59] G. Swartzlander, E. Ford, R. Abdul-Malik, L. Close, M. Peters, D. Palacios, and D. Wilson, "Astronomical demonstration of an optical vortex coronagraph," *Opt Express* **16**(14), 10200–10207 (2008).

- [60] C. Maurer, A. Jesacher, S. Bernet, and M. Ritsch-Marte, "What spatial light modulators can do for optical microscopy," *Laser & Photon Rev* **5**(1), 81–101 (2010).
- [61] L. Torner, J. P. Torres, and S. Carrasco, "Digital spiral imaging," *Opt Express* **13**(3), 873–881 (2005).
- [62] S. Fürhapter, A. Jesacher, S. Bernet, and M. Ritsch-Marte, "Spiral phase contrast imaging in microscopy," *Opt Express* **13**(3), 689–694 (2005).
- [63] S. Fürhapter, A. Jesacher, S. Bernet, and M. Ritsch-Marte, "Spiral interferometry," *Opt Lett* **30**(15), 1953–1955 (2005).